Strangeness conservation in hot nuclear fireballs

Jean Letessier and Ahmed Tounsi
Laboratoire de Physique Théorique et Hautes Energies, Université PARIS 7, Tour 24, 5è ét., 2 Place Jussieu, F-75251, Paris CEDEX 05, France

Ulrich Heinz and Josef Sollfrank
Institut für Theoretische Physik, Universität Regensburg D-93040 Regensburg, Germany

Johann Rafelski
Department of Physics, University of Arizona, Tucson, Arizona 85721
(Received 2 December 1992; revised manuscript received 21 October 1993)

Within a thermal model generalized to allow for nonequilibrium strange particle abundances we study how the constraint that the balance of strangeness in a fireball is (nearly) zero impacts the allowable thermal fireball parameters. Using the latest data of the CERN-WA85 experiment for the case of 200A GeV S-A ($A \sim 200$) collisions we extract the values of the thermal parameters considering in detail the impact of hadronic resonance decays on the abundances and spectral form of strange baryons and antibaryons. Given these results and invoking further the observed charged particle multiplicities we are able to consider the (specific) entropy content of the fireball in order to understand the nature of the disagreement of the hadronic gas picture of the fireball with the experimental data.

PACS number(s): 25.75.+r, 12.38.Mh, 24.85.+p

I. INTRODUCTION

Enhanced production of strange particles, and specifically of strange antibaryons, was suggested more than 10 years ago [1] as a possible signature for quark-gluon plasma (QGP) formation in relativistic nuclear collisions. This suggestion followed as a result of enhanced strange quark production, and therefore speedy equilibration of the strange quark flavor in the QGP and a large equilibrium strangeness density in the QGP phase. The (enhanced) production of (multi)strange antibaryons is considered to be more specifically related to deconfinement than are strange mesons, because of a large difference in chemical equilibration time scales [2] and chemical properties in the deconfined quark-gluon and hadronic-gas (HG) phases. These studies suggest further that if a QGP is not formed, its absence reveals itself by a relative suppression of strange compared to nonstrange particle production, similar to what is observed in usual hadron-hadron collisions. Detailed comparisons [3] of the expected strange particle yields arising from dynamical thermal systems consisting of a QGP and HG support this picture and have stimulated a number of experiments on strange particle production in nuclear collisions, related to the search for a QGP.

Recently several heavy-ion experiments [4] have reported a strong enhancement of all strange particle yields relative to proton-proton and proton-nucleus collisions, increasing with the centrality of the collision. The enhancement was seen particularly clearly in 200A GeV collisions of sulfur with various targets in the strange and multistrange baryon and antibaryon channels at central rapidity [5–8]. Furthermore, after accounting for resonance decay contributions [9], the momentum spectra of all secondary hadrons from these collisions [5,7,8,10] also show intriguing signs of thermalization and an onset of collective hydrodynamic flow [11], as would be expected for a high density "fireball" source of these particles. The key issue of this paper is the question as to what extent current data can help to distinguish between the direct formation of a fireball consisting of a dense and very hot hadron (resonance) gas [12–22] and the creation of a transient deconfined state such as the quark-gluon plasma (QGP) [19,20,22,23], followed by hadronization.[1]

In this analysis we concentrate the discussion on the strange hadron ratios from S-W collisions at 200A GeV [5,6] which can be combined with multiplicity data from the similar S-Pb collision system [24]. Because of the differences in baryon and energy stopping, the experimental results from the smaller S-S system at 200A GeV cannot be combined with the results analyzed here. However, we have recently also developed [25] a similar analysis of the central rapidity and global S-S data from NA35 [7,10] which, lacking information on multistrange baryons and antibaryons from this experiment, exploits data on nucleon, hyperon, and charged kaon production, with similar conclusions as the ones presented here.

[1]This work was originally submitted for publication prior to the release of the revised and more precise results [6] of the WA85 experiment. The full reanalysis here presented is reflecting all available information as of Summer 1993. See also note added in proof at the end of the manuscript.

Recent experimental results have already prompted several efforts to explain the observations in terms of the relatively simple framework of a thermal fireball model. The particular virtue of this approach is that the spectra and particle abundances can be described in terms of only a few macroscopic parameters. In perfect (local) thermodynamical equilibrium knowledge of the temperature $T(x)$, the chemical potentials $\mu_B(x)$ and $\mu_S(x)$ for the conserved baryon number and strangeness, respectively, and the velocity profile $u^\mu(x)$ for the collective expansion of the collision fireball are sufficient for a complete description of the final state — the values of these parameters at the hadronic freeze-out point determine the spectra and abundances of the observed particles. However, such a simple approach cannot *a priori* be expected to be successful. In particular the implicit assumption of complete chemical equilibrium is not necessarily consistent with the rapid dynamical evolution of the particle source. Kinetic arguments drive us to extend the simple fireball model by allowing for certain nonequilibrium features in the chemical composition of the fireball. We will show that the naive thermal model approach fails to describe the available data, and that such nonequilibrium extensions are required for a successful phenomenology.

Strangeness production processes constitute a bottleneck in chemical equilibration [1,2,26], and in our opinion even in a simple model one must account for a hierarchy of equilibration time scales in nuclear collisions: While thermal equilibration (which involves total cross sections) and chemical equilibration of the light quark flavors (which possess low pair production thresholds) occur fast, the production of strange quark pairs takes considerably more time in the HG phase where it is suppressed by high thresholds and small inelastic cross sections. In the HG phase there is in addition an intermediate time scale for the redistribution of the available strange quarks among all strange hadron channels: *Strangeness exchange* processes have in general low or vanishing thresholds and thus relatively large cross sections. This leads us to consider the notion of a final state in *relative chemical equilibrium* where all momentum spectra and nonstrange particle abundances are thermally and chemically equilibrated, and in particular the *relative* abundances of the strange hadrons have had time to reach a state of maximum entropy, but where the overall strangeness content is suppressed relative to its equilibrium value.

This necessitates the introduction of a strangeness saturation parameter $0 < \gamma_s \leq 1$ [19] which allows us to parametrize the effects of incomplete chemical equilibration of the strangeness sector. For a QGP state with its fast gluonic strangeness production even the natural short fireball lifetime of only a few fm/c should be sufficient to reach values of γ_s close to 1. In a purely hadronic fireball with its expected much longer strangeness saturation time scale small values of $\gamma_s \sim 0.1$ (such as those extracted from N-N collisions [25]) are much more likely. A measurement of γ_s thus in principle provides important information on the strangeness production time scale and hence on the possible structure of the collision fireball.

Another interesting nonequilibrium feature arises naturally when considering a scenario in which there was formation of an intermediate deconfined state. Very little is known about the time constants of hadronization; in particular one need not take for granted that the relative abundances of mesons and baryons, which may be produced by quite different hadronization mechanisms, obey the laws of relative chemical equilibrium. There may also be insufficient time for chemical equilibration of the meson and baryon components in the HG — processes which convert mesons into baryon-antibaryon pairs are generally relatively slow. A simple method to include the breaking of meson-baryon equilibrium will be discussed towards the end of Sec. IV where we will speculate about a possible early deconfined phase as source for the observed strange particles.

Strangeness conservation leads to a strong constraint on models of flavor evolution: The balance between s and $\bar{s}$ quarks requires nontrivial relations between the parameters of the models. These are in general difficult to satisfy and differ greatly in the different phases of strongly interacting matter — formally the QGP and HG phases of nuclear matter can be distinguished by their characteristically different behavior of the equilibrium strange quark chemical potential μ_s. In a strangeness neutral QGP fireball μ_s is exactly zero, independent of its temperature and baryon densities. In contrast with this, in any state consisting of locally confined hadronic clusters μ_s is generally different from zero at finite baryon density, in order to conserve strangeness. Only for the special case of baryon-free systems, i.e., $\mu_B = 0$, does the strange chemical potential vanish at any T, due to particle-antiparticle symmetry. At nonzero baryon density $\mu_B \neq 0$, there is just one special value $T(\mu_B)$ for which $\langle s \rangle = \langle \bar{s} \rangle$ at $\mu_s^{\rm HG} = 0$. This temperature is bounded from above by a limiting value $T_{s\ \rm max}$ which generally depends on the detailed form of the equation of state (EOS). For the case of a conventional (Hagedorn-type) HG these values have been studied previously [13,14,20]. We find here that there is some sensitivity of $T_{s\ \rm max}$ to the form of the hadronic gas spectrum, regarding specifically the inclusion of the maximum number of known states. Use of all known hadronic resonances rather than only the ground state octets and baryon decuplet (which in general biases the spectrum in favor of nonstrange particles over strange particles) *decreases* the value of the temperature $T_{s\ \rm max}$ from $\simeq$ 225 to $\simeq$ 200 MeV.

The theoretical study of strangeness conservation and its relationship to the condition $\mu_s = 0$, which is natural for the deconfined state, constitutes the main body of Sec. II. We will consider, for various temperature regions relevant to present and future heavy-ion experiments, the relationship between the strange quark chemical potential μ_s and the baryon chemical potential μ_B in the HG phase. At $T \simeq 200$ MeV one observes in the HG the peculiar feature that $\mu_s(\mu_B)$ stays close to zero over a relatively large range of μ_B [20,21]. We also consider the impact of a given (small) fraction of net strangeness in the fireball, $\varepsilon \equiv \langle \bar{s} - s \rangle / \langle s \rangle \ll 1$, which can arise due to fluctuations in particle emission.

Within the thermal model, γ_s and μ_s of the particle

source can be obtained from the measured strange particle ratios [19]. One striking result of our present analysis of the WA85 data [5,6], confirmed by the analysis [25] of the NA35 data [7], is the finding of a vanishing strange quark potential $\mu_s \simeq 0$ with a rather high accuracy. The analysis of the WA85 data is developed in Sec. III with considerable sophistication, including in particular the effects of resonance decays and collective flow on the particle ratios, confirming the result $\mu_s \simeq 0$ for a variety of different freeze-out scenarios.

Combining this apparently rather stable result with the earlier discussion of strangeness neutrality, we immediately run into a series of problems with the interpretation of the data in terms of an equilibrated hadron gas: A literal interpretation of the inverse slope of the transverse mass spectra as the source temperature, $T = 232$ MeV, is excluded because then the strangeness neutrality condition cannot be satisfied [the discrepancy amounts to 2.5 standard deviations (s.d.)] and at such high temperatures the hadron gas cannot be considered as an ensemble of noninteracting particles. Furthermore, since such an interpretation would exclude the existence of collective transverse flow, the freeze-out condition would be strongly violated.[2] Restoration of strangeness neutrality requires the introduction of transverse collective flow: Interpreting the inverse transverse slope in terms of a freeze-out temperature $T_f = 190$ MeV blueshifted by a transverse flow velocity $\beta_f = 0.20$, we recover strangeness neutrality of the HG. This does not, however, improve much the problems with the internal consistency of the noninteracting hadron gas picture and with the freeze-out condition, since the amount of flow is too low [11]. Also, as will be discussed in Sec. IV, such an interpretation fails to reproduce the data on the total and net charged multiplicity densities by about 3 s.d. — introducing even more flow, namely, $\beta_f = 0.41$, allows one to reduce the fireball temperature to a value of $T_f = 150$ MeV which is consistent with the freeze-out criterium [11], renders the hadron gas sufficiently dilute to remove the internal consistency problems, and is also compatible with lattice QCD restrictions [27] on the critical temperature for the transition into a QGP. This interpretation also happens to correctly reproduce the total and net charged multiplicity data. However, in this scheme the strangeness neutrality condition is now broken in the opposite direction by about 4 s.d., as measured by the discrepancy between the measured and required strange quark chemical potential.

None of these three scenarios gives a natural explanation of the observed large amount of strangeness saturation, $\gamma_s = 0.7$–0.8. A conventional HG does not seem to provide a sufficiently long lifetime to achieve such a degree of saturation, and also recent two-pion interferometry data [28] show no evidence at all for a sufficiently long-lived hadronic (i.e., pion-emitting) source.

[2]With the previously published data [5], which indicated a somewhat lower temperature and a larger baryon density, the strangeness neutrality problem could be avoided [20,21], but not the consistency and freeze-out problems.

In order to allow for future experiments to shed more light on the nature of the fireball at freeze-out, we present a number of predictions for the production of other strange and nonstrange hadrons, based on the above picture of a hadronic state in *relative chemical equilibrium* for a variety of freeze-out scenarios. These predictions are quantitative for the S-W collision system at $200A$ GeV, and can serve as a qualitative guide for the yet unexplored Pb-Pb collisions (for which within our approach we cannot, however, predict precisely the temperature and chemical potentials). We have already alluded to the fact that the HG picture appears to have another problem when compared to the data, namely, that it does not reproduce the large measured charged multiplicities. In Sec. IV we discuss how within the HG framework data on total and net charged multiplicities can be translated into a measure of the specific entropy $\sigma \equiv \mathcal{S}/\mathcal{B}$ of the fireball. At fixed (e.g., measured) temperature and chemical potential the specific entropy is a characteristic quantity which distinguishes a HG from a deconfined state of quarks and gluons [20,22]: It is much larger in the QGP phase, $\sigma_Q(T,\mu_B) > \sigma_H(T,\mu_B)$, due to the excitation of the abundant gluon degrees of freedom. We explore how the easily measurable ratio of net charge density to total charged multiplicity density,

$$D_Q \equiv \frac{\frac{dN^+}{dy} - \frac{dN^-}{dy}}{\frac{dN^+}{dy} + \frac{dN^-}{dy}}\,, \tag{1}$$

is related to the (inverse) of the specific entropy, extending the work of Ref. [22] by including all resonance decays. Since the relationship is nearly the same with and without strange particles present in the calculations we believe the relation between specific entropy and D_Q is rather insensitive to the detailed flavor composition of the observed hadronic system. For this and other similar reasons we think that D_Q is a very valuable observable from which semiquantitative information about entropy can be gained even if the source of hadron radiation is a hadronizing quark-gluon plasma or some other novel form of matter.

Calculating D_Q from the HG with chemical parameters extracted from the strange particle production data, we find that the HG does not reproduce sufficient total multiplicity to explain the data from experiment EMU05 [24]. This was already argued by us before [22], but our present analysis takes into account a significant recent change in the experimental strange particle data [6], and corrects earlier calculational inaccuracies. These developments reduce considerably the discrepancy between the ensemble of experimental results and a HG fireball, but we are still left with a 3.5 s.d. effect. Because of the relative smallness of this difference we have made a considerable effort here considering, e.g., off-equilibrium states, in order to find some HG-based model which might resolve this discrepancy, but the incompatibility remains and is a further strong indication that a HG in-

terpretation of the data is not possible.

What then is the nature of the particle-emitting source? At this point one might be inclined to give up the concept of thermal and chemical equilibrium altogether. However, the beautiful thermal phenomenology of the hadronic momentum spectra [11] and the intriguing stability of the vanishing strange chemical potential combined with a large amount of strangeness saturation (which are confirmed by other heavy-ion experiments at CERN [25], but differ strongly from N-N phenomenology [25] at the same energy and from heavy-ion results at the lower energy reached at the BNL Alternating Gradient Synchrotron (AGS) [29]) prompt us to speculate in the rest of the paper about a hadronizing QGP as the possible source of the observed particles. Although on the basis of existing data we are not able to come to definite conclusions in this paper, this possibility raises interesting questions which motivate further theoretical and experimental studies.

While $\mu_s = 0$ is natural for the deconfined state, this value could be in principle compatible with other forms of hadronic matter in which mesons are the dominant carriers of the strange flavor, but we are not aware of such a model. These arguments can also be used to advance a chirally symmetric hadronic phase in which all hadronic masses are lower than considered here: Although an in-depth analysis is hampered by the lack of reliable equations of state for such a scenario, it is natural to expect a behavior between QGP and HG phases for many observables. But even in such a "chiral" scenario the value of $\mu_s \simeq 0$ remains an accidental mystery, since strangeness conservation at finite baryon density would in general again lead to a nonzero strange chemical potential. However, we note that other attempts to explain the enhanced strange antibaryon production have invoked very strong medium modifications of the masses in the hadron gas [30] and the formation of color ropes with unusually strong color electric fields [31]. All these approaches imply rather violent modifications of conventional hadron physics and form, in our opinion, just another way of stating its breakdown and postulating new physics. In neither case have compatibility of the models with the global reaction picture and the different detailed characteristics of the experiments such as $\mu_s \simeq 0$, $\gamma_s \sim 1$, which we address, been demonstrated.

Our paper is organized as follows. In Sec. II we present our thermal model with special attention given to the thermal parameters describing the approach to relative chemical equilibrium. We investigate the importance of the u-d asymmetry and study the condition of strangeness balance in a HG. In Sec. III we extract the thermodynamic parameters from the WA85 data on strange baryon and antibaryon production, taking into account hadronic resonance decays and transverse and longitudinal flow. In Sec. IV the implications of the extracted thermal parameters for the entropy content of the fireball and for the charged particle multiplicity are discussed. We also explore a parametrization of a hadronizing QGP state regarding the agreement with the data. In Sec. V we discuss the implications of our results for the nature and dynamical evolution of the fireball.

II. THERMAL MODELS

The use of thermal models to interpret data on particle abundances and spectra from nuclear collisions is motivated by the hope and expectation that in collisions between sufficiently large nuclei at sufficiently high energies a state of excited nuclear matter close to local thermodynamic equilibrium can be formed, allowing us to study the thermodynamics of QCD and the possible phase transition from a HG to a QGP at a critical energy density. Since we do not yet reliably know how big the collision system and how large the beam energy have to be for this to occur (if at all), thermal models should be considered as a phenomenological tool to test for such a behavior. Even if successful, the validity of such an approach must be checked later by a more detailed theoretical analysis of the kinetic evolution of the collision fireball.

Much of our analysis will be carried out assuming a specific form of the equation of state. For the hadronic gas state we follow in this paper the conventional hadronic gas model first developed by Hagedorn *et al.* [32] in which the equation of state of any hadronic system is obtained from a partition function which sums over all hadronic resonances. It is believed that by including a complete set of intermediate scattering states in the form of (usually zero-width) hadronic resonances the dominant interactions within the hadronic system are automatically taken into account. However, an important, but tacit approximation, is made in this approach, concerning the parameters such as mass (and sometimes widths) of the resonances which are inserted with their free space values. This neglects the possibility that in particular at high temperature and particle or baryon density, there may occur significant shifts from the free space values — one often speaks in this context of the melting of hadronic masses as one approaches extreme conditions. The standard hadronic gas model is certainly not sufficiently precise for our purpose if we were to ask questions concerning the absolute values of energy, entropy, baryon density, etc., which strongly depend either on the ever increasing mass spectrum of particles or on the proper volume occupied by the particles [33]. On the other hand the condition of zero strangeness and quantities such as the entropy per baryon, which involve ratios of extensive variables, are independent of the absolute normalization of the volume and of the renormalization introduced by the diverging particle spectrum and hence can safely be considered in our approach.

When considering the properties of the deconfined phase we shall employ the perturbative QCD result for quarks and gluons with strong interactions taken into account up to first order in the coupling constant α_s. Details of these equations of state can be found in numerous references; see, e.g., [3,16].

A. Fireball parameters

We assume that in collisions between two nuclei a region with nearly thermal equilibrium conditions is formed near "central" rapidity, i.e., at rest in the center-of-

momentum frame of the projectile and a target tube with the diameter of the projectile. This central fireball from which the observed particles emerge is described by its temperature T and by the chemical potentials, which we shall discuss below. The temperature is conventionally extracted from the inverse slope of the experimental transverse mass spectra at central rapidity. However, if at "freeze-out" (where the particles cease to interact) the source expands collectively with a transverse flow velocity β_f, this inverse slope is governed by a superposition of random thermal and collective flow motion. Except at low $p_\perp$, "flow spectra" resemble purely thermal spectra [11], with an asymptotic slope at high $m_\perp$ corresponding to an apparent "blueshifted" temperature:

$$T_{\rm app} = T_f \sqrt{\frac{1+\beta_f}{1-\beta_f}} \,. \tag{2}$$

The separation of the two contributions, i.e., the isolation of T_f, from the experimental value $T_{\rm app}$ is not straightforward, but has been attempted in [11] exploiting in particular slight differences in how flow affects particles of different mass, and by requiring consistency with the freeze-out kinetics. Such studies favor a rather low freeze-out temperature $T_f \simeq 150$ MeV and attribute the remainder of the slope to flow. We note that experimentally $T_{\rm app} \sim 235$ MeV.

As we shall see, the particle abundance ratios determine the ratios μ_i/T_f of the chemical potentials to the temperature at freeze-out, independent of the amount of flow and of the absolute value of the temperature. There are two independent chemical potentials for baryon number and strangeness conservation, μ_B and μ_S. These have been used in [18,21,23]. Alternatively, and more conveniently for our purposes, one can use the quark chemical potentials μ_q and μ_s for light and strange quarks, respectively. This in no way assumes quark deconfinement, but merely recognizes the fact that in the quark model the quantum numbers of hadrons are obtained by adding the quantum numbers of their constituent quarks. One can further account for isospin conservation by distinguishing between up and down quarks, introducing separate chemical potentials μ_u and μ_d (see Sec. II B).

The relationship between the two sets of chemical potentials is given by

$$\begin{aligned} \mu_q &= \mu_B/3 \,, \\ \mu_s &= \mu_B/3 - \mu_S \,, \\ \mu_S &= \mu_q - \mu_s \,, \end{aligned} \tag{3}$$

where the minus signs are due to the conventional assignment of strangeness -1 to the strange quark. If B_h, S_h are the baryon number and strangeness of hadron h, its chemical potential can thus be written either as

$$\mu_h = B_h\,\mu_B + S_h\,\mu_S \tag{4}$$

in terms of μ_B and μ_S, or as

$$\mu_h = \nu_h^q \mu_q + \nu_h^s \mu_s \,, \tag{5}$$

where ν_h^q, ν_h^s count the number of light and strange valence quarks inside the hadron, respectively, with antiquarks counted with a minus sign.

As mentioned the particle numbers are more directly given in terms of the fugacities, related to the chemical potentials by

$$\lambda_i = e^{\mu_i/T} \,. \tag{6}$$

The fugacity of each hadronic species is simply the product of the valance quark fugacities, viz., $\lambda_p = \lambda_u^2 \lambda_d$, $\lambda_{K^+} = \lambda_u \lambda_{\bar{s}}$, etc. Since the strong and electromagnetic interactions do not mix the quark flavors u, d, and s, these are separately conserved on the time scale of hadronic collisions and can only be produced or annihilated in particle-antiparticle pairs. In *absolute chemical equilibrium* with respect to these pair creation processes the chemical potentials for particles and antiparticles are opposite to each other, implying, for the respective fugacities,

$$\lambda_{\bar{i}} = \lambda_i^{-1} \,. \tag{7}$$

If absolute equilibrium in the strange sector is not reached, a convenient way of parametrizing this effect is by introducing a common saturation factor $0 < \gamma_s \leq 1$ for both strange quarks and antiquarks. Their abundance is then regulated by the effective fugacities

$$\begin{aligned} \lambda_s^{\rm eff} &= \gamma_s \lambda_s \,, \\ \lambda_{\bar{s}}^{\rm eff} &= \gamma_s \lambda_s^{-1} \,, \end{aligned} \tag{8}$$

and the relation (7) between the particle and antiparticle fugacities is preserved. Following Eqs. (5) and (6) the individual hadron fugacities λ_h are then given by a product of valence quark fugacities,

$$\lambda_h = \Pi_j \, \lambda_j \,, \tag{9}$$

and the approach to equilibrium is controlled by the factor

$$\gamma_h = \gamma_s^{n(h,s)} \,, \tag{10}$$

where the power $n(h,s)$ counts the total number of valence strange quarks *plus* antiquarks in the hadron species h. This parametrization takes into account that once a strange-antistrange quark pair has been created its redistribution among the various strange hadronic species is no longer hindered by thresholds and occurs relatively fast. It thus makes sense to introduce the concept of a HG in *relative chemical equilibrium*, in which the strange phase space is not fully saturated (viz., $\gamma_s \neq 1$), but strangeness has been distributed among the available strange hadron channels according to equilibrium fugacities in order to maximize the entropy.

Up to this point the fireball is thus described by the following six thermal parameters: the freeze-out temperature T_f and its freeze-out radial velocity β_f, its baryon chemical potential μ_B, the strange quark chemical potential μ_s, the light quark asymmetry potential $\delta\mu$ (see Sec. II B), and the strangeness saturation factor γ_s.

The number of independent variables can be, however,

reduced by considering theoretically the u-d asymmetry in the fireball and relating it to the asymmetry potential $\delta\mu$, and by the condition of strangeness conservation which can be used to fix μ_s — this leaves us with four parameters (e.g., T_f, β_f, μ_B, γ_s). Among the four, the spectral form is most sensitively related to T_f and β_f, while μ_B and γ_s control the relative particle abundances. The thermal parameters enter the thermodynamic description through the partition function from which all observables are derived.

We now look more closely at the theoretical constraints which limit the number of free thermal parameters in the fireball.

B. u-d asymmetry

In our calculations we will distinguish between the u and d quarks by introducing separate fugacities λ_u and λ_d, substituting them for λ_q in the partition function as appropriate. For exact u-d symmetry we can revert to the previous notation via

$$\mu_q = (\mu_d + \mu_u)/2 \ . \tag{11}$$

Here μ_q is the "light quark" chemical potential ($\mu_B/3$ in terms of the baryon chemical potential). Since even in the heaviest nuclei the neutron excess causes only a small u-d asymmetry, the difference

$$\delta\mu = \mu_d - \mu_u \tag{12}$$

is generally small. We also define the light flavor ratio between the net number of down and up quarks in the fireball:

$$R_f = \frac{\langle d - \bar{d} \rangle}{\langle u - \bar{u} \rangle} \ . \tag{13}$$

In a central S-W collisions, where a tube with the transverse area of the S projectile is swept out from the W target and participates in the fireball, one has $R_f^{\text{S-W}} \simeq 1.08$; in Pb-Pb collisions $R_f^{\text{Pb-Pb}} = 1.15$. The value of $\delta\mu$ is at each fixed T determined by the value of R_f, but depends on the assumed structure of the source, i.e., the EOS. We have investigated this relation for the two cases considered here: the conventional HG and the QGP.

In the HG phase we include in the partition function all mesons and baryons up to 2 GeV mass [34], adding the only known $\Omega(2250)$ resonance. Higher resonances would matter only if their number were divergent (as is the case in the Bootstrap approach of Hagedorn *et al.* [32]) *and* if the HG was sufficiently long lived to populate them all. Strange hadrons are included as described in Eq. (16) below, with λ_q replaced by $\lambda_{u,d}$ as appropriate if the system is not isospin symmetric.

In Fig. 1 we show how in the conventional hadron gas the difference $\delta\mu/\mu_q$ induced by the isospin asymmetry of the fireball depends on the temperature, for the two selected values $R_f = 1.08$ and 1.15 discussed above, and for three fixed values of $\lambda_s = 0.95$, 1.00, and 1.05. The curves shown correspond to the nontrivial solutions (i.e., solutions with $\mu_q \neq 0$) of the strangeness balance equation with the given values for λ_s; as we will explain below, these solutions cease to exist (since we require $\langle s - \bar{s} \rangle \simeq 0$) above a certain critical temperature, which is given by $T_{s\ \max} \simeq 200$ MeV for $\lambda_s = 1$ and decreases (increases) for smaller (larger) values of λ_s. We see that, while for $T \to 0$ the ratio $\delta\mu/\mu_q$ vanishes in the hadron gas, it is of the same order as the deviation from unity of R_f once T reaches values around 150–200 MeV which are of interest here.

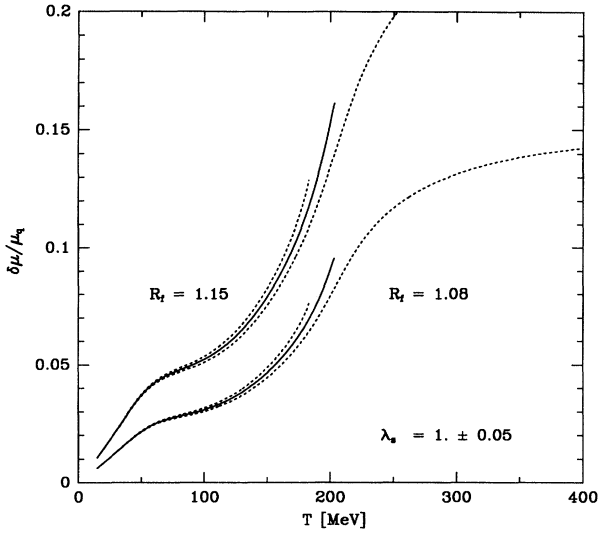

FIG. 1. Isospin asymmetry $\delta\mu/\mu_q$ for $R_f = 1.08$ (S-W collisions) and $R_f = 1.15$ (Pb-Pb collisions). Solid lines, $\lambda_s = 1.00$; upper dotted lines, $\lambda_s = 1.05$; lower dotted lines, $\lambda_s = 0.95$.

For the QGP EOS, the ratio $\delta\mu/\mu_q$ is independent of λ_s, due to the decoupling of the strange and nonstrange chemical potentials in the partition function. For $\mu_q < \pi T$ one finds [19]

$$R_f^{\text{QGP}} \simeq \frac{\mu_d}{\mu_u} \simeq 1 + \frac{\delta\mu}{\mu_q} , \tag{14}$$

such that $\delta\mu/\mu_q$ is exactly equal to $R_f^{\text{QGP}} - 1$. It is remarkable that towards the maximum temperature consistent with strangeness conservation the HG- and QGP-based results for $\delta\mu$ at a given R_f nearly agree. We thus find that, although small, the difference between the chemical potentials of u and d quarks is not always negligible. We note for later applications that in the region of interest to us here ($T \sim 150$–200 MeV) we have irrespective of the nature of the fireball:

$$\frac{\delta\mu}{T} \approx \frac{\mu_q}{T}(R_f - 1) \ . \tag{15}$$

C. Strangeness partition function

In the Boltzmann approximation, it is easy to write down the partition function for the strange particle frac-

tion of the hadronic gas, $\mathcal{Z}_s$, and we follow the notation of Ref. [14], except for including a larger set of strange particles and resonances. Including the possibility of an only partially saturated strange phase space through the factor γ_s above, but suppressing for simplicity the isospin asymmetry $\delta\mu$, we have

$$\ln \mathcal{Z}_s^{\rm HG} = \frac{V_h T^3}{2\pi^2}\Big[(\lambda_s\lambda_q^{-1}+\lambda_s^{-1}\lambda_q)\gamma_s F_K + (\lambda_s\lambda_q^2+\lambda_s^{-1}\lambda_q^{-2})\gamma_s F_Y + (\lambda_s^2\lambda_q+\lambda_s^{-2}\lambda_q^{-1})\gamma_s^2 F_\Xi + (\lambda_s^3+\lambda_s^{-3})\gamma_s^3 F_\Omega\Big], \tag{16}$$

where all kaon (K), hyperon (Y), cascade (Ξ), and omega (Ω) resonances plus their antiparticles are taken into account. The phase space factors F_i of the various strange particle families are

$$F_K = \sum_j g_{K_j} W(m_{K_j}/T)\,,$$

$$K_j = K, K^*, K_2^*, \ldots, \quad m \le 1780 \text{ MeV}\,,$$

$$F_Y = \sum_j g_{Y_j} W(m_{Y_j}/T)\,,$$

$$Y_j = \Lambda, \Sigma, \Sigma(1385), \ldots, \quad m \le 1940 \text{ MeV}\,,$$

$$F_\Xi = \sum_j g_{\Xi_j} W(m_{\Xi_j}/T)\,,$$

$$\Xi_j = \Xi, \Xi(1530), \ldots, \quad m \le 1950 \text{ MeV}\,,$$

$$F_\Omega = \sum_j g_{\Omega_j} W(m_{\Omega_j}/T)\,, \quad \Omega_j = \Omega, \Omega(2250)\,. \tag{17}$$

The g_i are the spin-isospin degeneracy factors, $W(x) = x^2 K_2(x)$, and K_2 is the modified Bessel function.

For the quark-gluon plasma, on the other hand, the strange contribution to the partition function is much simpler, because the strange quarks and antiquarks are isolated and do not occur in clusters with nonstrange quarks as in the hadron gas:

$$\ln \mathcal{Z}_s^{\rm QGP} = \frac{g_s V}{2\pi^2}\int p^2\,dp\,[\ln(1+\gamma_s\lambda_s e^{-\sqrt{m_s^2+p^2}/T}) + \ln(1+\gamma_s\lambda_s^{-1}e^{-\sqrt{m_s^2+p^2}/T})]\,, \tag{18}$$

with the strange quark spin-color degeneracy factor

$$g_s = 2\times 3 = 6\,. \tag{19}$$

For the value of the strange quark mass (usually considered range 150–180 MeV) we take, in Eq. (18), $m_s = 160$ MeV; we note that the coefficients γ_s and λ_s do not factorize as has been the case for the hadron gas, because for $T \simeq m_s$ the Boltzmann approximation is not always satisfactory and can produce errors of the order of 20% in Eq. (18). Recall that in general the strange particle density in a QGP is larger by a factor 2–5 than in a HG, due to the lower threshold ($m_s < m_K$) and the presence of the color degeneracy factor in Eq. (19).

D. Strangeness balance

We will now discuss the reduction of the number of free parameters caused by the condition of strangeness balance. Since the net strangeness of the colliding nuclei in the initial state is zero, and strangeness is conserved by strong interactions, the net strangeness of the collision fireball will stay close to zero throughout the collision, except for a possible strangeness asymmetry in surface radiation of strange hadrons [13,37] (strangeness distillation) which could arise during QGP hadronization. Distillation is thought to occur when chemical equilibrium is enforced during a slow QGP hadronization process. The associated phase diagram and the strangeness balance conditions for systems with (large) finite net strangeness are presented elsewhere [35].

The condition of vanishing total strangeness takes the form

$$0 = \rho_s = \langle s\rangle - \langle\bar{s}\rangle = \lambda_s\frac{\partial}{\partial\lambda_s}\ln\mathcal{Z}_s\,, \tag{20}$$

where ρ_s is the net strangeness density,

$$\rho_s = \sum_i s_i\rho_i\,, \tag{21}$$

with s_i being the strangeness of particle species i having density ρ_i, and the sum going over all particle species i existing in the respective phase (QGP or HG). While for the QGP this relation leads always to the result $\lambda_s = 1$ or $\mu_s = 0$ [as one easily verifies by inserting Eq. (18)], for the hadron gas it is an implicit equation relating λ_s to λ_q in a way which depends on the temperature T [13,14].

In order to be certain that our conclusions do not sensitively depend on exact conditions of strangeness balance, but also in order to be able to account for surface emission fluctuations, we introduce the net strangeness fraction

$$\varepsilon \equiv \frac{\langle\bar{s}\rangle - \langle s\rangle}{\langle s\rangle}\,, \tag{22}$$

and will also consider solutions for the analogue of Eq. (20), where the left hand side is given by $-\varepsilon\langle s\rangle$. In this work we consider asymmetries $|\varepsilon| \le 0.1$ which should occasionally arise as result of purely statistical fluctuations caused by surface emission. We note briefly the practical consequences of $\varepsilon = \pm 0.1$: For the fireball created in central S-W collisions one has about 108 baryons in the interaction tube. If we consider a hadron gas with the thermal parameters (without flow component) as determined for the S-W collision data [20], we

find a strange pair abundance of about 0.4 per baryon or about 40 strange pairs in total. The maximum asymmetry considered here in the HG phase at $T \simeq 200$ MeV is thus about ± 4 strange quarks. Fluctuations in surface emission leading to such a breaking of strangeness neutrality in the remaining fireball can be expected to occur in about half of the collision systems.

1. Condition $\mu_s = 0$ ($\lambda_s = 1$)

Since the vanishing of μ_s for all values of T and μ_B in a strangeness-neutral QGP appears to be such a unique feature of this state, it is interesting to ask to what extent this characteristic value could arise in a HG as well. Of course, for a baryon-free system ($\mu_B = 0$) $\mu_s = 0$ is a natural consequence of strangeness neutrality even in the hadron gas. For systems with nonvanishing baryon number [like the central rapidity fireballs created at AGS and CERN Super Proton Synchrotron (SPS) energies] this is no longer true. We therefore ask under which conditions $\mu_s = 0$, viz., $\lambda_s = 1$, allows for nonzero values of μ_B^0 to be consistent with strangeness neutrality. This issue can be resolved analytically: Inserting the partition function (16) into the strangeness neutrality condition (20), we see that at $\lambda_s = 1$ the phase space for Ω and $\overline{\Omega}$ cancels out, giving the exact result

$$\mu_B^0 = 3T \operatorname{arccosh}\left(\frac{F_K}{2F_Y} - \gamma_s \frac{F_\Xi}{F_Y}\right) . \qquad (23)$$

Real solutions exist only when the argument on the right hand side is larger than unity. It turns out that this condition is a sensitive function of the temperature T and of the hadronic resonance spectrum included in the F_i. For any given resonance mass spectrum, there is a temperature $T_{s\,\max}$ beyond which no such solution is possible — this occurs since F_K/F_Y is a monotonically decreasing function of T (see Fig. 1 in Ref. [14]).

The case of exact strangeness neutrality ($\varepsilon = 0$) in a HG in absolute chemical equilibrium ($\gamma_s = 1$) was considered in [21], and in this special case our following analysis agrees with their work. However, as shown in the following section, the new experimental data are in clear disagreement with such a simple model. One can easily generalize the result Eq. (23) to include a small net strangeness and/or to allow small nonvanishing values of the strange quark chemical potential. An important result is that there is a domain of temperatures near $T = 200$ MeV for which even a considerable change of μ_B between $\mu_B = 0$ and μ_B^0 does not induce a significant change of $\mu_s \simeq 0$. The characteristic temperature where this occurs depends only weakly on the values γ_s, μ_s, and ε, as long as their deviations from the canonical values are not too large. For example, taking into account all known resonances up to a mass of 2 GeV, we find that this behavior occurs at $T \simeq 200$ MeV for $\varepsilon = 0$ and at $T \simeq 190$ MeV for $\varepsilon = -0.1$. When the number of hadronic resonances is reduced by a factor 2 by cutting the spectrum off at 1.6 GeV, this temperature increases by about 15 MeV.

We illustrate the situation in Figs. 2(a) and 2(b), where we present the constraint between μ_s and μ_B at fixed $T =$ 200 MeV (solid curves), 150 MeV (long-dashed curves), 300 MeV (short-dashed curves), and 1000 ($\simeq \infty$) MeV (dotted curves) for $\varepsilon = 0$ computed with mass spectrum of resonances up to 1.6 GeV [Fig. 2(a)] and up to 2 GeV [Fig. 2(b)]. We see that the larger set of resonances leads to a small reduction in the value of μ_s at fixed μ_B, T, of the order of 8 MeV at the maxima of the curves. We further see that for $\mu_B \sim 200$ MeV at $T = 200$ MeV the strangeness-neutral state is found for $\mu_s = 0$; for $\mu_B \sim$ 300 MeV, which we will see applies to the experimental

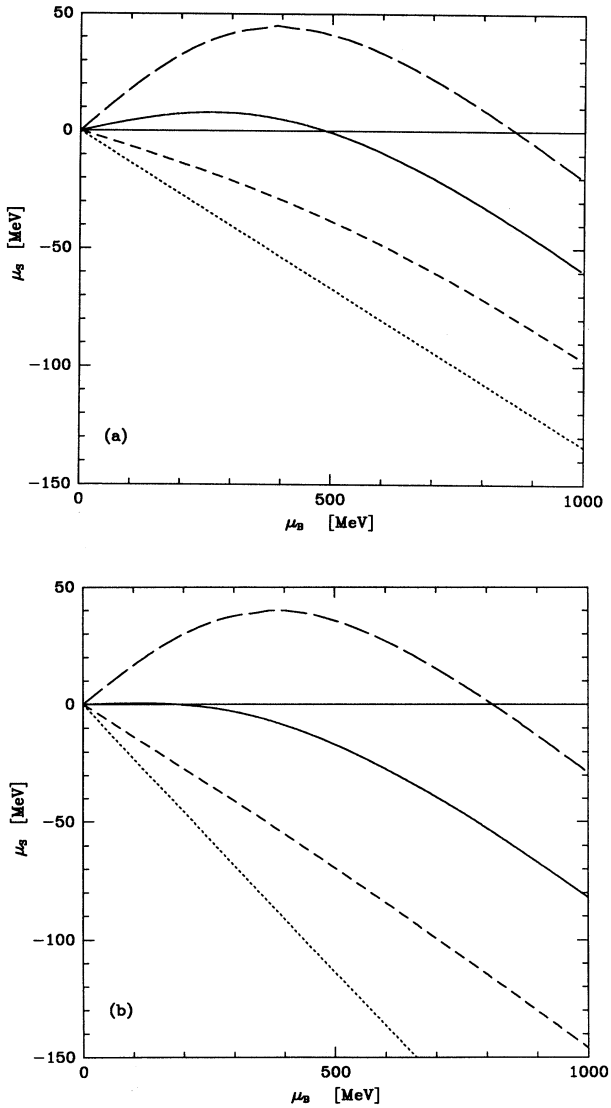

FIG. 2. Strange quark chemical potential μ_s versus baryon chemical potential μ_B in a strangeness neutral HG. In (a) a smaller set of hadronic resonances was used as compared to (b) (see text). The long-dashed line corresponds to $T = 150$ MeV, the solid line to $T = 200$ MeV, and the dashed line to $T = 300$ MeV. The dotted line is the limiting curve for large T, computed here at $T = 1000$ MeV. The horizontal solid line corresponds to $\mu_s(\mu_B) = 0$ (independent of T) in a strangeness-neutral QGP.

situation at CERN, one can estimate already from these figures that the strangeness neutrality is found at $T = 190$ MeV. Similar results hold for the cases $\varepsilon = \pm 0.1$, with negative (positive) ε acting to reduce (increase) the temperature at which $\mu_s \simeq 0$ by $\delta T \sim 10$ MeV. We note that these and other calculations we present are carried out at $\gamma_s = 0.7$, which is justified by the experimental results. However, in this instance the choice $\gamma_s = 1$ would not visibly modify our results.

The flat behavior of μ_s as a function of μ_B for $T \simeq 200$ MeV makes it hard to distinguish the hadron gas from a QGP (which has $\mu_s \equiv 0$ independent of μ_B) around the temperature T_f=190 MeV. This peculiar property of the Hagedorn-type hadronic gas was first pointed out in Ref. [21]. Our analytical result Eq. (23) and the corresponding Figs. 2(a) and 2(b) explain the origin of this effect and allow us to understand the accidental nature of this behavior. We stress that this "indistinguishibility" of the HG and QGP, based on strangeness conservation for $\mu_s = 0$ in both phases, happens only in a small window of temperatures, which is below the apparent temperatures extracted from the transverse spectra from S-W collisions at SPS energies, and it is present only as long as we pretend that strangeness production differences between the QGP and HG are not an important factor.

III. ANALYSIS OF THE DATA WITHIN THE FIREBALL MODEL

It has been noted repeatedly that, especially in collisions involving heavy nuclear targets, the observed particle spectra, after correcting for resonance decay effects [9], resemble thermal distributions with a common inverse slope (apparent temperature) T. This slope parameter can be understood [see Eq. (2)] in terms of thermal motion plus collective flow, with the true temperature being significantly lower, but appearing blueshifted by the collective expansion of the source [11]. It was observed in [19] that the observed particle ratios appear to be consistent with a generalized thermal model, which assumes equilibration only of the momentum distributions and the light quark abundances, but allows for *deviations* in particle abundances *from absolute chemical* equilibrium in the strange sector arising from incomplete occupation of the accessible strangeness phase space.

In this section we will reanalyze the detailed information on strange baryon and antibaryon production obtained by the experiment WA85 [5,6]. We will first review shortly the approximate analytical scheme developed in [19] and then expand it numerically to include the effects of resonance decays and collective flow. We find in Secs. III A–III C that the simple analytical discussion gives remarkably accurate results, especially if the true temperature of the emitting system is not above $\sim$ 190 MeV. For $T \sim T_{\rm app} \sim 232$ MeV resonance production is very significant, and their decays cannot be neglected. However, they mainly affect the extraction of the strangeness saturation factor γ_s (inclusion of resonance decays drives the extracted γ_s closer to 1, i.e., towards full saturation of the HG phase space), while the extracted fugacities, in particular the vanishing strange quark chemical potential, are remarkably stable against resonance decays and temperature variations due to transverse flow.

A. Cancellation of the Boltzmann factor

It was argued in [19] that within the thermal model it is quite easy to extract the fugacities from a given particle ratio *at fixed* $m_\perp$ *and* y, thus eliminating the need to extrapolate the experimental data to full phase space. Specifically, for a stationary fireball one finds for the ratio of particles i and j, for each of which the invariant cross section is experimentally known at a certain rapidity $y \pm dy/2$ in the region $m_\perp \geq m_\perp^{\rm cut}$:

$$\left.\frac{dN_i/dy}{dN_j/dy}\right|_{m_\perp \geq m_\perp^{\rm cut}} = \frac{g_i\,\gamma_i\,\lambda_i}{g_j\,\gamma_j\,\lambda_j}\,\frac{\int_{m_\perp^{\rm cut}}^{\infty} m_\perp \cosh y\, \exp(-m_\perp \cosh y/T)\, dm_\perp^2}{\int_{m_\perp^{\rm cut}}^{\infty} m_\perp \cosh y\, \exp(-m_\perp \cosh y/T)\, dm_\perp^2}\,. \tag{24}$$

Here we used the identity $E = m_\perp \cosh y$ for the particle energy (with y measured relative to the center of mass of the collision fireball) to rewrite the transverse mass integral over the Boltzmann distribution $E\,\exp(-E/T)$ (the factor E results from starting with the Lorentz-invariant cross section $E\,d^3N/d^3p$). If the fireball is not stationary, but expands in the longitudinal direction in a boost-invariant way, dN/dy is independent of y, and the factors $E\,\exp(-E/T)$ under the integrals on the right-hand side (RHS) of Eq. (24) have to be replaced by a Bessel function [11]:

$$\frac{dN_i^{\rm thermal}}{dy\,dm_\perp^2} = g_i\,\gamma_i\,\lambda_i\,m_\perp\,K_1\left(\frac{m_\perp}{T}\right), \tag{25}$$

where we neglected a common normalization constant containing the fireball volume which drops out from the ratio. We note that the same result is obtained if the spectrum in Eq. (24) is integrated over rapidity, i.e., if one wants to describe data obtained over a relatively large rapidity window — longitudinal flow effectively widens the acceptance in rapidity of an experiment. The important observation is here that obviously in both cases the Boltzmann factors (and with them all dependence on the particle rest masses) drop out from the ratio, due to the common lower cutoff on $m_\perp$ (which, of course, must be larger than either rest mass). The same remains true if $m_\perp$ is not integrated over, but the ratio is evaluated at fixed $m_\perp$. Since the degeneracy factors g_i are known, this immediately yields the ratio of the generalized fugacities $\gamma_i\lambda_i$ [see Eq. (10)].

B. Extraction of μ_s and μ_q from antibaryon data

Thus, comparing the *spectra* of particles with those of their antiparticles within overlapping regions of $m_\perp$, the Boltzmann and *all* other statistical factors cancel from their relative normalization, which is thus a function of the equilibrium fugacities only. In Sec. III D we show that this statement still remains approximately valid when feed-down by resonance decays is included. For the available two such ratios in experiment WA85 one has specifically

$$R_\Xi = \frac{\overline{\Xi^-}}{\Xi^-} = \frac{\lambda_d^{-1}\lambda_s^{-2}}{\lambda_d\lambda_s^2}\ , \tag{26}$$

$$R_\Lambda = \frac{\overline{\Lambda}}{\Lambda} = \frac{\lambda_d^{-1}\lambda_u^{-1}\lambda_s^{-1}}{\lambda_d\lambda_u\lambda_s}\ . \tag{27}$$

These ratios can easily be related to each other, in a way which shows explicitly the respective isospin asymmetry factors and strangeness fugacity dependence. Equations (26) and (27) imply

$$R_\Lambda R_\Xi^{-2} = e^{6\mu_s/T}e^{2\delta\mu/T}\ , \tag{28}$$

$$R_\Xi R_\Lambda^{-2} = e^{6\mu_q/T}e^{-\delta\mu/T}\ . \tag{29}$$

Equations (28) and (29) are generally valid, irrespective of the state of the system (HG or QGP), as long as the momentum spectra of the radiated particles are "thermal" with a common temperature (inverse slope). We see that once the left hand side is known experimentally, it determines rather accurately the values of μ_q, μ_s which enter on the right hand side with a dominating factor 6, while the (small) isospin asymmetry $\delta\mu$ plays only a minor role. This explains how, by applying these identities to the early WA85 data [5], it has been possible [19] to determine the chemical potentials with considerable precision in spite of the still relatively large experimental errors on the measured values of R_Λ, R_Ξ.

Turning to the pertinent experimental results we first recall the recently released data on the rapidity dependence of $\overline{\Lambda}$ and Λ production rates measured by the experiment NA36 [8]. There is a clear indication that the production of these particles in nuclear S-Pb collisions is concentrated in the central rapidity domain — it does not follow in its behavior the FRITIOF simulations which, on the other hand, are consistent with the production rates from p-Pb collisions. This supports the notion of a central fireball reaction picture also for the S-W collisions studied by WA85 [5,6]. The most striking result of the latter experiment is the fact that the abundance of charged anticascades ($\bar{s}\bar{s}\bar{d}$) is unusually enhanced, in particular when compared to the abundance of cascades (ssd) and antilambdas ($\bar{s}\bar{u}\bar{d}$). We will now interpret the data in terms of the local equilibrium model, thus fixing the values of μ_s and μ_q.

We shall use in this analysis the revised more precise data [6] presented at the *Quark Matter '93* meeting in early summer 1993. These differ in some critical detail from the values published before.[3] The $\overline{\Xi^-}/\Xi^-$ ratio is

$$R_\Xi = 0.41 \pm 0.05$$

$$\text{for } y \in (2.3, 2.8) \text{ and } m_\perp > 1.9 \text{ GeV}. \tag{30}$$

Note that, in p-W reactions, in nearly the same $(p_\perp, y)$ region, a smaller value for the R_Ξ ratio, namely, 0.27 ± 0.06, is found. The $\bar{\Lambda}/\Lambda$ ratio is[4]

$$R_\Lambda = 0.20 \pm 0.01$$

$$\text{for } y \in (2.3, 2.8) \text{ and } m_\perp > 1.9 \text{ GeV}. \tag{31}$$

In Eq. (31), corrections were applied to eliminate hyperons originating from cascade decays. The ratio R_Λ for S-W collisions is comparable to p-W collision results in the same kinematic range.

From these two results, together with Eqs. (28), (29), and (15), and the value $R_f = 1.08$ mentioned after Eq. (13), we obtain the following values of the chemical potentials for S-W central collisions at 200A GeV:

$$\frac{\mu_q}{T} = \frac{\ln R_\Xi/R_\Lambda^2}{5.94} = 0.39 \pm 0.04\,, \tag{32}$$

$$\frac{\delta\mu}{T} = \frac{\mu_q}{T}(R_f - 1) = 0.031 \pm 0.003\,, \tag{33}$$

$$\frac{\mu_s}{T} = \frac{\ln R_\Lambda/R_\Xi^2 - 0.062}{6} = 0.02 \pm 0.05\,. \tag{34}$$

We will see that these qualitative results are in good agreement with the more detailed numerical evaluation given below. The last result translates into the value $\lambda_s = 1.02 \pm 0.05$ for the strange quark fugacity (compared to the exact value 1.03 ± 0.05). Much of what we do later in this paper will rest on this stunning result that the strange chemical potential is very small and entirely compatible with zero.[5] In our calculations below we will thus consider in particular a HG constrained to this range of values (as well as to near strangeness neutrality).

In order to obtain absolute values for the chemical potentials we need to know the temperature of the source. A study of the apparent temperatures (inverse $m_\perp$ slopes) in S-A collisions at SPS was made. Leaving aside possible flow effects, the maximum temperature allowed by the data of $T = 232 \pm 5$ MeV would lead to the following chemical potentials:

---

[3] In the originally preprinted version of this paper we used the older and less precise data [5] which were also consistent with our fireball model, albeit at different values for the chemical potentials.

[4] This value has changed by 2.5 (old) standard deviations and is now given much more precisely.

[5] The old data [5] yielded nearly the same strange chemical potential, namely, $\mu_s/T = -0.02 \pm 0.05$, but a considerably larger baryon chemical potential, $\mu_q/T = 0.53 \pm 0.1$.

$$\mu_B = 275 \pm 10 \text{ MeV}\ , \quad \delta\mu = 7.2 \pm 0.7 \text{ MeV}\ ,$$
$$\mu_s = 4.5 \pm 12 \text{ MeV}\ . \tag{35}$$

In the presence of transverse flow the temperature would be lower, resulting in a proportional reduction of the chemical potentials.

C. Determination of γ_s

A complete cancellation of the fugacity factors occurs when we form the product of the abundances of baryons and antibaryons. We further can take advantage of the cancellation of the Boltzmann factors by comparing this product for two different particle kinds; e.g., we consider

$$\Gamma_s \equiv \left.\frac{\Xi^-}{\Lambda}\frac{\overline{\Xi^-}}{\overline{\Lambda}}\right|_{m_\perp > m_\perp^{\rm cut}} . \tag{36}$$

If the phase space of strangeness, like that of the light flavors, were fully saturated, the fireball model would imply $\Gamma_s = 1$. However, any deviation from absolute chemical equilibrium as expressed by the factor γ_s will change the value of Γ_s. Ignoring at present the feed-down effects from higher resonances we find

$$\Gamma_s = \gamma_s^2 . \tag{37}$$

In principle the measurement of γ_s can be done with other particle ratios; in the absence of resonance feed-down we have

$$\gamma_s^2 = \left.\frac{\Lambda}{p}\frac{\overline{\Lambda}}{\overline{p}}\right|_{m_\perp > m_\perp^{\rm cut}} = \left.\frac{\Xi^-}{\Lambda}\frac{\overline{\Xi^-}}{\overline{\Lambda}}\right|_{m_\perp > m_\perp^{\rm cut}} = \left.\frac{\Omega^-}{2\Xi^-}\frac{\overline{\Omega^-}}{2\overline{\Xi^-}}\right|_{m_\perp > m_\perp^{\rm cut}} , \tag{38}$$

where in the last relation the factors 2 in the denominator correct for the spin-3/2 nature of the Ω. As we will see in Sec. III E, these double ratios are considerably affected by resonance decays. We note that in the kinematic domain of Eqs. (30) and (31) the experimental results reported by the WA85 collaboration are

$$\frac{\overline{\Xi^-}}{\overline{\Lambda} + \overline{\Sigma^0}} = 0.4 \pm 0.04\,, \qquad \frac{\Xi^-}{\Lambda + \Sigma^0} = 0.19 \pm 0.01\,. \tag{39}$$

If the mass difference between Λ and Σ^0 is neglected, this implies in the framework of the thermal model that an equal number of Λ's and Σ^0's are produced, such that

$$\frac{\overline{\Xi^-}}{\overline{\Lambda}} = 0.8 \pm 0.08\,, \qquad \frac{\Xi^-}{\Lambda} = 0.38 \pm 0.02\,. \tag{40}$$

The fact that the more massive and stranger anticascade practically equals at fixed $m_\perp$ the abundance of the antilambda is most striking. These results are inexplicable in terms of simple cascade models for the heavy-ion collision [38]. The relative yield of $\overline{\Xi^-}$ is 3.5 times greater than seen in the p–p experiment at the CERN Intersecting Storage Rings (ISR) [39] and all other values reported in the literature, which amounts to a 4 s.d. effect [5,6]. Combining the experimental result Eq. (40) with Eqs. (36) and (37), we find the value

$$\gamma_s = 0.55 \pm 0.04\,. \tag{41}$$

We shall see that in a full analysis which accounts for resonance formation and decays, in particular when allowing for flow, this result moves to $\gamma_s = 0.7$–0.8. However, we find it impossible to adjust the amount of flow to approach the full equilibrium value $\gamma_s = 1$ to less than 3 s.d.; this shows clearly the incompatibility of the data with the naive hadronic gas model investigated in [21,23]. On the other hand, given the general prejudices about strangeness equilibration time scales in a HG environment, the observed value of $\gamma_s = 0.7$–0.8 is still surprisingly large, especially if compared to the much smaller value $\gamma_s \simeq 0.2$ characterizing N-N reactions [25]. It indicates the presence of new, unexpectedly fast strangeness equilibration mechanisms in nuclear collisions. We believe that a systematic investigation of the observable Γ_s in Eq. (36) as a function of the geometric size of the interaction region and of the collision energy is needed in order to clarify the mechanisms for this fast approach to strangeness equilibrium.

D. Temperature, flow, and transverse mass spectra

The recent data from the WA85 collaboration [5,6] correspond to an apparent temperature (from the slope of the $m_\perp$ spectra) of $T_{\rm app} = 232 \pm 5$ MeV in the central rapidity interval $2.3 < y < 2.8$. This value is extracted by fitting the data with a thermal distribution without transverse flow as described in Sec. III A. If the slope of the experimental spectra is not entirely due to thermal motion, but contains a flow component due to collective expansion of the emitting source [11], then "flow spectra" (i.e., boosted Boltzmann spectra) have to be used in the numerator and denominator of Eq. (24). If the flow is azimuthally symmetric and boost invariant in the longitudinal direction, the thermal spectrum Eq. (25) has to be replaced by (neglecting a common normalization constant)

$$\frac{dN_i^{\rm flow}}{dy\, dm_\perp^2} = g_i\, \gamma_i\, \lambda_i\, m_\perp\, K_1\left(\frac{m_\perp \cosh\rho}{T}\right) I_0\left(\frac{p_\perp \sinh\rho}{T}\right) , \tag{42}$$

where K_1 and I_0 are the modified Bessel functions and

$$\rho = \text{arctanh}\beta_f \tag{43}$$

is the transverse flow rapidity. This spectrum has an asymptotic slope corresponding to an apparent "blue-shifted" temperature given in Eq. (2).

The same result as in Eq. (42) is obtained if the spectrum from a spherically expanding fireball is integrated over rapidity. Since some longitudinal flow is likely to be present in S-W collisions, and also the kinematic window of the WA85 experiment is half of a rapidity unit,

we think that the form, Eq. (42), in which integration over a large rapidity window is implied, is most appropriate for an analysis of the experimental spectra. (The "large window" combines the acceptance in WA85 with about 1.5 units of flow expected [11] for this system.) Because of the dependence on $m_\perp$ and $p_\perp$ in Eq. (42) there is no exact cancellation of the spectral shape from the $m_\perp$-integrated particle ratios, and their independence from the $m_\perp$ cut mentioned in Sec. III A is lost as well. This renders the analysis of the data and extraction of the thermal parameters (fugacities, etc.) in general more complicated.

E. Resonance decays

As already mentioned, Eq. (24) is only correct if feed-down to the observed particles by strong decays of higher resonances is neglected. At $T \sim 200$ MeV these resonance decays can no longer be totally ignored. This has two annoying consequences: First, since the decay products have a steeper $m_\perp$ spectrum than the original resonances [9], the various contributions to numerator and denominator in Eq. (24) have different slopes, and the integrals over the Boltzmann factors no longer cancel exactly. Second, since different sets of resonances contribute to i and j, the ratio is modified by an *a priori* unknown factor which turns out to be hard to calculate and in general *does* depend on the experimental $m_\perp$ cutoff as well as on the temperature.

Since the decay spectra drop more steeply as a function of $m_\perp$ than the thermal ones, the role of resonance feed-down can in principle be suppressed by going to sufficiently large $m_\perp$. For pions and kaons, for example, the thermal contribution dominates for $m_\perp > 1$–1.5 GeV, in spite of the huge contribution of decay pions to the total yield [9]; these all end up at lower $m_\perp$. For baryons due to their larger masses, the difference in slope between the thermal and decay baryons is less drastic, and one has to go to still larger $m_\perp$ before the resonance decay contributions are sufficiently suppressed.

Including resonance decays, the numerator and denominator of Eq. (24) take the form

$$\left.\frac{dN_i}{dy}\right|_{m_\perp \geq m_\perp^{\rm cut}} = \int_{m_\perp^{\rm cut}}^{\infty} dm_\perp^2 \left\{ \frac{dN_i^{\rm thermal/flow}(T)}{dy\, dm_\perp^2} + \sum_R b_{R\to i} \frac{dN_i^R(T)}{dy\, dm_\perp^2} \right\}, \tag{44}$$

with the direct thermal or flow contribution given by Eq. (25) or Eq. (42), respectively, and the contribution from decays of resonances $R \to i + 2 + \cdots + n$ (with branching ratio $b_{R\to i}$ into the observed channel i) calculated according to Ref. [9]:

$$\frac{dN_i^R}{dy\, dm_\perp^2} = \int_{s_-}^{s_+} ds\, g_n(s) \int_{Y_-}^{Y_+} dY \int_{M_\perp^-}^{M_\perp^+} dM_\perp^2 \left(\frac{dN_R}{dY\, dM_\perp^2}\right) \times \frac{M}{\sqrt{P_\perp^2 p_\perp^2 - [ME^* - M_\perp m_\perp \cosh(Y-y)]^2}}\,. \tag{45}$$

Capital letters indicate variables associated with the resonance R, $\sqrt{s}$ is the invariant mass of the unobserved decay products $2, \ldots, n$, and the kinematic limits are given by

$$s_- = \left(\sum_{k=2}^{n} m_k\right)^2, \qquad s_+ = (M - m_i)^2, \tag{46}$$

$$Y_\pm = y \pm \operatorname{arcsinh}\frac{p^*}{m_\perp}, \tag{47}$$

$$M_\perp^\pm = M \frac{E^* m_\perp \cosh(Y-y) \pm p_\perp \sqrt{p^{*2} - m_\perp^2 \sinh^2(Y-y)}}{m_\perp^2 \sinh^2(Y-y) + m_i^2}, \tag{48}$$

$$E^* = \frac{1}{2M}(M^2 + m_i^2 - s), \qquad p^* = \sqrt{E^{*2} - m_i^2}. \tag{49}$$

In Eq. (45), $g_n(s)$ is the decay phase space for the n-body decay $R \to i + 2 + \cdots + n$, and for the dominant two-body decay (assuming isotropic decay in the resonance rest frame) it is given by

$$g_2(s) = \frac{1}{4\pi p^*}\, \delta(s - M^2), \tag{50}$$

for $n > 2$ (see [9]).

The resonance spectrum $dN_R/dy\, dM_\perp^2$ entering the RHS of Eq. (45) is in general itself a sum of a thermal or flow spectrum like Eq. (25) or Eq. (42) and of decay spectra from still higher-lying resonances; for example, most decays of high-lying nucleon resonances into protons or antiprotons proceed through the $\Delta(1232)$ or its antipar-

ticle [e.g., $N(1440) \to \Delta(1232) + \pi \to p + 2\pi$]. This has been taken into account in our calculations. Extracting the degeneracy factors and fugacities of the decaying resonances, we write shortly

$$N_i^R \equiv \gamma_R \lambda_R \tilde{N}_i^R \equiv \gamma_R \lambda_R \int_{y \text{ window}} dy \int_{m_\perp^{\rm cut}}^{\infty} dm_\perp^2 \times \sum_R g_R \, b_{R\to i} \frac{d\tilde{N}_i^R}{dy \, dm_\perp^2} , \quad (51)$$

with the sum now including only resonances with identical quantum numbers; if these quantum numbers agree with those of species i, the sum is meant to also include the thermal contribution.

Between particles and antiparticles we have the relation

$$N_{\bar{i}}^{\bar{R}} = \gamma_R \, \lambda_R^{-1} \, \tilde{N}_i^R = \lambda_R^{-2} \, N_i^R . \quad (52)$$

The three independent particle ratios measured by WA85 [5,6] are thus given by

$$R_\Xi = \left. \frac{\overline{\Xi^-}}{\Xi^-} \right|_{m_\perp \geq m_\perp^{\rm cut}} = \frac{\gamma_s^2 \lambda_q^{-1} \lambda_s^{-2} \tilde{N}_\Xi^{\Xi^*} + \gamma_s^3 \lambda_s^{-3} \tilde{N}_\Xi^{\Omega^*}}{\gamma_s^2 \lambda_q \lambda_s^2 \tilde{N}_\Xi^{\Xi^*} + \gamma_s^3 \lambda_s^3 \tilde{N}_\Xi^{\Omega^*}} , \quad (53)$$

$$R_\Lambda = \left. \frac{\overline{\Lambda}}{\Lambda} \right|_{m_\perp \geq m_\perp^{\rm cut}} = \frac{\lambda_q^{-3} \tilde{N}_\Lambda^{N^*} + \gamma_s \lambda_q^{-2} \lambda_s^{-1} \tilde{N}_\Lambda^{Y^*} + \gamma_s^2 \lambda_q^{-1} \lambda_s^{-2} \tilde{N}_\Lambda^{\Xi^*}}{\lambda_q^3 \tilde{N}_\Lambda^{N^*} + \gamma_s \lambda_q^2 \lambda_s \tilde{N}_\Lambda^{Y^*} + \gamma_s^2 \lambda_q \lambda_s^2 \tilde{N}_\Lambda^{\Xi^*}} , \quad (54)$$

$$R_s = \left. \frac{\Xi^-}{\Lambda} \right|_{m_\perp \geq m_\perp^{\rm cut}} = \frac{\gamma_s^2 \lambda_q \lambda_s^2 \tilde{N}_\Xi^{\Xi^*} + \gamma_s^3 \lambda_s^3 \tilde{N}_\Xi^{\Omega^*}}{\lambda_q^3 \tilde{N}_\Lambda^{N^*} + \gamma_s \lambda_q^2 \lambda_s \tilde{N}_\Lambda^{Y^*} + \gamma_s^2 \lambda_q \lambda_s^2 \tilde{N}_\Lambda^{\Xi^*}} . \quad (55)$$

$\tilde{N}_\Lambda^{Y^*}$ contains also (in fact as its most important contribution) the electromagnetic decay $\Sigma^0 \to \Lambda + \gamma$. We have not included the (small) effect of the weak decay $\Omega \to YK$ since this contamination should be eliminated by experimental cuts. If the right hand sides are evaluated using Eqs. (44), (45), and (51) with $m_\perp^{\rm cut} = 1.9$ GeV, for the left hand sides the experimental values (30), (31), and (39) can be inserted, and Eqs. (53), (54), and (55) can be solved for γ_s, λ_s, and λ_q. Note that we do not distinguish here between λ_u and λ_d since this would require the calculation of a separate decay cascade for each member of an isospin multiplet. The smallness of $\delta\mu$ in Eq. (33) justifies this approximation.

F. Fireball parameters and particle yields

1. *Values of the thermal model parameters*

We now proceed to determine numerically the values of the thermal parameters which were introduced in the analytical discussion in Secs. III B and III C. The precise results of our analysis are given in Table I, including the full error progression arising from the uncertainties in the input particle ratios. We present in the table three cases.

(A) A thermal model without flow, $\beta_f = 0$, where the temperature T_f is assumed to correspond directly to the value $T_{\rm app} = 232$ MeV following from the

TABLE I. Thermal fireball parameters extracted from the WA85 data [6] on strange baryon and antibaryon production, for three different interpretations of the measured $m_\perp$ slope. Resonance decays were included. For details see text.

	(A) "thermal" $T = 232$ MeV, $\beta_f = 0$	(B) "thermal and flow" $T = 150$ MeV, $\beta_f = 0.41$	(C) strangeness balance $T = 190$ MeV, $\beta_f = 0.20$
λ_s	1.03 ± 0.05	1.03 ± 0.05	1.03 ± 0.05
μ_s/T	0.03 ± 0.05	0.03 ± 0.05	0.03 ± 0.05
μ_s (MeV)	7 ± 11	4 ± 7	6 ± 9
λ_q	1.49 ± 0.05	1.48 ± 0.05	1.48 ± 0.05
μ_q/T	0.40 ± 0.04	0.39 ± 0.04	0.39 ± 0.04
μ_B (MeV)	278 ± 23	176 ± 15	223 ± 19
γ_s	0.69 ± 0.06	0.79 ± 0.06	0.68 ± 0.06
ϵ	−0.22	0.37	0
$\mathcal{S}/\mathcal{B}$	18.5 ± 1.5	48 ± 5	26 ± 2.5
D_Q	0.135 ± 0.01	0.08 ± 0.01	0.12 ± 0.01

slope of the transverse mass spectra of high-$m_\perp$ strange (anti)baryons.

(B) A model with a freeze-out temperature of $T_f = 150$ MeV, i.e., a value consistent with the kinetic freeze-out criterion developed in [11] and with lattice QCD data on the phase transition temperature, which entails a flow velocity at freeze-out of $\beta_f = 0.41$.

(C) In order to maintain zero net strangeness in the HG fireball at relative chemical equilibrium between strange meson and baryon abundances, we consider the case $T_f = 190$ MeV with $\beta_f = 0.20$.

Since the probability to excite the various resonances contributing to the observed final particle abundances depends on T_f, it is not surprising that slightly different values of the chemical parameters result from the same data in the three different scenarios. Comparing the numerical results of Table I with the simple analytical approximation Eqs. (32), (34), and (41), which contained only a rough estimate of the radiative Σ^0 decay but no contributions from higher resonances, we can draw the following conclusions.

(1) The extraction of λ_q and λ_s according to Eqs. (26) and (27) is only very weakly affected by resonance decays and by the origin of the slope of the $m_\perp$ spectrum (thermal or flow). (The absolute value of the associated chemical potentials does, of course, depend on the choice of the freeze-out temperature.) The reason is that in Eq. (53) [Eq. (54)] the first [second] term in the sums occurring in the numerator and denominator completely dominates. Taking the results for the "thermal" scenario ($T_f = 232$ MeV) from Table I and evaluating with them the $\overline{\Xi^-}/\Xi^-$, $\overline{\Lambda}/\Lambda$, and Ξ^-/Λ ratios excluding the contributions from higher resonances changes them by -2%, -7%, and $+31\%$, respectively (leaving out also the $\Sigma^0 \to \Lambda\gamma$ contribution totally changes the Ξ^-/Λ ratio by 115%).

(2) Since the Ξ^-/Λ ratio is the crucial ingredient for the determination of the strangeness saturation factor γ_s, the effects from resonance decays and flow can be clearly seen in this number. From Eq. (40) we had extracted [cf. Eq. (41)] $\gamma_s = 0.55 \pm 0.04$; improving this simple factor 2 estimate for the Σ^0 contribution by its correct thermal weight would have lowered this value — however, consideration of the decay of higher-lying resonances raises γ_s, and we obtain at $T_f = 232$ MeV, the value $\gamma_s = 0.69 \pm 0.06$; cf. Table I. Taking conditions with conserved strangeness [case (C) with $T = 190$ MeV and $\beta_f = 0.2$] has not much impact — but at a low freeze-out temperature of $T = 150$ MeV with $\beta_f = 0.41$ [case (B)] we find an increase to $\gamma_s = 0.79 \pm 0.06$; both results are inconsistent with the equilibrium $\gamma_s^{\rm eq} = 1$.

(3) The conclusion of [19] that the WA85 data on strange baryon and antibaryon production from 200A GeV S-W collisions establish a vanishing strange quark chemical potential is confirmed; this result is stable against large variations in the temperature and transverse flow velocities with their implied considerable changes in the excitation and decay of high mass resonances. This finding will serve as the cornerstone of the following studies in Sec. IV. Note that also the light quark fugacity is practically unaffected by the complex pattern of resonance formation and decay as well as by the amount of transverse flow in the spectra.

It is clear that the extraction of three thermodynamic parameters (λ_q, λ_s, and γ_s) from three independent particle ratios [the forth value presented by WA85 is related by the simple algebraic relation; cf. Eq. (56) below] cannot be considered a very convincing test of the generalized thermal model considered here, in particular since the extracted values depend on the choice of the temperature whose independent derivation from the shape of the $m_\perp$ spectrum is not model independent, and since the theoretical consistency arguments of Ref. [11] which prefer the lower temperature of around 150 MeV lead to a situation where strangeness conservation in the fireball is not automatically guaranteed. It is therefore mandatory that our model receive further experimental tests in the form of measurements of other independent particle ratios, see note added in proof. We note that several additional particle ratios, in particular those involving Ω, $\overline{\Omega}$ and p, $\bar{p}$, are expected to become soon available from the WA94 Collaboration [6,40] in a kinematic region compatible with the WA85 results. We draw here attention to the very preliminary report [6] of the central rapidity abundance of $\overline{\Omega} = 4 \pm 2$ and $\Omega = 7 \pm 3.6$ which can be used to form a ratio since the experimental acceptances are the same for both particles. This result implies $\overline{\Omega}/\Omega \simeq 0.6 \pm 0.4$ which is compatible with the prediction shown in Table II (see discussion below). This prediction is extremely sensitive to the fireball character of the model and to the value of λ_s: $\overline{\Omega}/\Omega = \lambda_s^{-6}$, which implies $\lambda_s = 1.1^{+0.2}_{-0.1}$.

2. *Transverse mass spectra*

We present, in Fig. 3, the $m_\perp$ spectra of the various particle species of interest here, computed for two scenarios (I) for the "thermal" scenario, [Figs. 3(a) and 3(b)] with $T = 232$ MeV, $\beta_f = 0$, $\lambda_q = 1.49$, $\lambda_s = 1.03$, $\gamma_s = 0.69$; p, $\bar{p}$, Λ, $\overline{\Lambda}$ [Fig. 3(a)]; Ξ, $\overline{\Xi}$, Ω, $\overline{\Omega}$ [Fig. 3(b)]; (II) for the hadronic kinetic freeze-out scenario with flow, with $T = 150$ MeV, $\beta_f = 0.41$, $\lambda_q = 1.48$, $\lambda_s = 1.03$, $\gamma_s = 0.79$ [Figs. 3(c) and 3(d)]; p, $\bar{p}$, Λ, $\overline{\Lambda}$ [Fig. 3(c)]; Ξ, $\overline{\Xi}$, Ω, $\overline{\Omega}$ [Fig. 3(d)]. Dashed lines marked "th" indicate the direct thermal contribution to the spectra, while the solid lines marked "tot" include in addition all resonance decay contributions. In order to separate the yields of particles and antiparticles shown in Figs. 3(a)–3(d) we have multiplied the latter yield by a factor 0.1. The presence of flow affects the spectra mostly at low $m_\perp$ near the mass threshold [11], where it leads to a flattening, i.e., to a higher apparent temperature. The effect is proportional to the particle mass (since for small $p_\perp$ the effect of flow can be estimated by $p_{\rm flow} \simeq m_0 v_{\rm flow}$) and thus most obvious in the Ξ^- and Ω spectra.

These results comprise several resonance decays with the exception of the Ω and its antiparticle — there are effectively no resonance contributions since only the very heavy $\Omega(2250)$ is known and has been considered here. While the overall common normalization of all spectra is arbitrary, their relative normalization is highly significant and in general characteristic for the model employed.

TABLE II. Input (*) and predicted high-$m_\perp$ particle ratios for the S-W 200A GeV collisions. The parameters for the three "thermal," "thermal and flow," and "balanced strangeness" scenarios are as specified in Table I.

$N_i/N_j\Big\vert_{m_\perp^{\rm cut}=1.9\,{\rm GeV}}$	(A) "thermal"	(B) "thermal and flow"	(C) "strangeness balance"
$\overline{\Xi^-}/\Xi^-$	0.41 ± 0.05*	0.41 ± 0.05*	0.41 ± 0.05*
$\overline{\Lambda}/\Lambda$	0.20 ± 0.01*	0.20 ± 0.01*	0.20 ± 0.01*
Ξ^-/Λ	0.19 ± 0.01*	0.19 ± 0.01*	0.19 ± 0.01*
$\overline{\Xi^-}/\overline{\Lambda}$	0.40 ± 0.04*	0.40 ± 0.04*	0.40 ± 0.04*
Λ/p	0.60 ± 0.06	0.62 ± 0.06	0.59 ± 0.06
$\overline{\Lambda}/\overline{p}$	1.2 ± 0.1	1.2 ± 0.1	1.2 ± 0.1
Ω^-/Ξ^-	0.53 ± 0.05	0.29 ± 0.03	0.45 ± 0.04
$\overline{\Omega^-}/\overline{\Xi^-}$	1.1 ± 0.1	0.60 ± 0.06	0.94 ± 0.09
Ω^-/Λ	0.10 ± 0.02	0.05 ± 0.01	0.08 ± 0.02
$\overline{\Omega^-}/\overline{\Lambda}$	0.42 ± 0.08	0.23 ± 0.05	0.36 ± 0.07
$\overline{\Omega^-}/\Omega^-$	0.85 ± 0.25	0.85 ± 0.25	0.85 ± 0.25
$\overline{p}/p$	0.10 ± 0.02	0.10 ± 0.02	0.10 ± 0.02
K^-/K^+	0.53 ± 0.08	0.51 ± 0.08	0.53 ± 0.08

We immediately notice that the two scenarios considered here could be distinguished more easily if we knew the relative yields of omegas to cascades or hyperons (and their antiparticles), with the most notable observation that the $\overline{\Omega}$ yield is predicted to be near to $\overline{\Xi}$ yield at fixed $m_\perp$ for the flow scenario, and is even larger for the thermal scenario. We will next see that in principle it is possible to distinguish the flow model cases (A), (B), and (C) using multistrange-baryon abundances. Recent reports [6] (see above) allow us to expect that sufficiently precise relative yields of Ω and $\overline{\Omega}$ will be soon available.

3. *Particle ratios*

When the transverse mass spectra are integrated over $m_\perp$ one obtains the particle multiplicity in a given rapidity window. As discussed in Sec. III A, the analysis within a thermal model should be based on particle ratios with a common minimum $m_\perp$ for the integral. In the experiment WA85 the most recent results are given for $m_\perp^{\rm cut} = 1.9$ GeV. In our analysis we have chosen $m_\perp^{\rm cut}$ to be a parameter in order to show how the particle ratios depend on the cutoff of the acceptance. In this way we explore in our calculations the consequences (for both the "thermal" and "flow" scenarios) of an increase of the experimental acceptance towards lower transverse momenta. This allows to better compare results of different experiments with different acceptances.

We present in Figs. 4(a)–4(d) the particle ratios as function of $m_\perp^{\rm cut}$, for the two cases considered in Fig. 3. The solid curves are obtained without flow, $T = 232$ MeV, and the dashed curves with $T_f = 150$ MeV, $\beta_f = 0.41$. The crosses indicate the experimental input data used to fix the parameters of the model and display the experimental error. Comparing $m_\perp$-integrated particle ratios with different $m_\perp$ cuts gives an idea of the effects coming from the somewhat different slopes of thermally emitted particles and resonance decay products. We notice that the particle ratios available so far from the WA85 experiment are both insensitive to the amount of flow present and almost insensitive to the value of $m_\perp^{\rm cut}$—remarkably the slight model dependence which can be barely observed in the ratios of Ξ/Λ and $\overline{\Xi}/\overline{\Lambda}$ ratios just disappears for $m_\perp^{\rm cut} = 1.9$ GeV.

On the other hand we note that the ratios involving omegas (which are under analysis in WA85) are sensitive both to the model temperature and the value of $m_\perp^{\rm cut}$. This is a natural consequence of the fact that all baryons have a considerable number of cascading resonances contributing noticeably to their abundance, with the exception of the omegas. Consequently, in any particle ratio involving Ω or $\overline{\Omega}$ we see the dependence on temperature and $m_\perp^{\rm cut}$ of the resonance contributions to the other particle yields. As the temperature drops, the dominant feature is a drop in the yield of Ω and $\overline{\Omega}$. At fixed T, as $m_\perp^{\rm cut}$ increases we see the fading of the cascading resonance contributions to the other particle abundance in the ratio. This very interesting result, however, demands some caution: The effective absence of resonance decay contributions to the Ω spectrum in our calculation could be impacted by the discovery of so far unknown Ω^* resonances. We also recall that the large Ω/Ξ^- and (in particular) $\overline{\Omega}/\overline{\Xi^-}$ ratios are in part due to the additional spin degeneracy of the spin-3/2 Ω.

From Fig. 4(a) we further see that for K^- and K^+

the decay contributions differ at finite μ_B, leading to an appreciable upward curvature of the particle ratio at low $m_\perp^{\rm cut}$, particularly strongly visible for the high temperature case. One sees a flattening towards high $m_\perp^{\rm cut} >$ 1.5–2 GeV, where the direct thermal component dominates. We refrain here from a comparison between abundances of mesons to baryons, as we are uncertain, also in view of the deviation of γ_s from the equilibrium value, whether it is prudent to assume that the relative meson to baryon abundance follows the thermal equilibrium ratio (see Sec. IV). We summarize our findings about particle ratios with $m_\perp^{\rm cut}$ in Table II and draw attention to the errors in the prediction arising from full propagation of the error in the experimental particle ratio input values. Ratios, at high $m_\perp$, which are insensitive to the scenario, such as $\bar{p}/p$, $\overline{\Omega}/\Omega$, Λ/p, $\overline{\Lambda}/\bar{p}$, K^-/K^+, should be seen as consistency tests of the model here developed; the other ratios involving either Ω or $\overline{\Omega}$ will help deconvolute in the apparent temperature the flow and thermal components. Ratios involving protons should be taken with a grain of

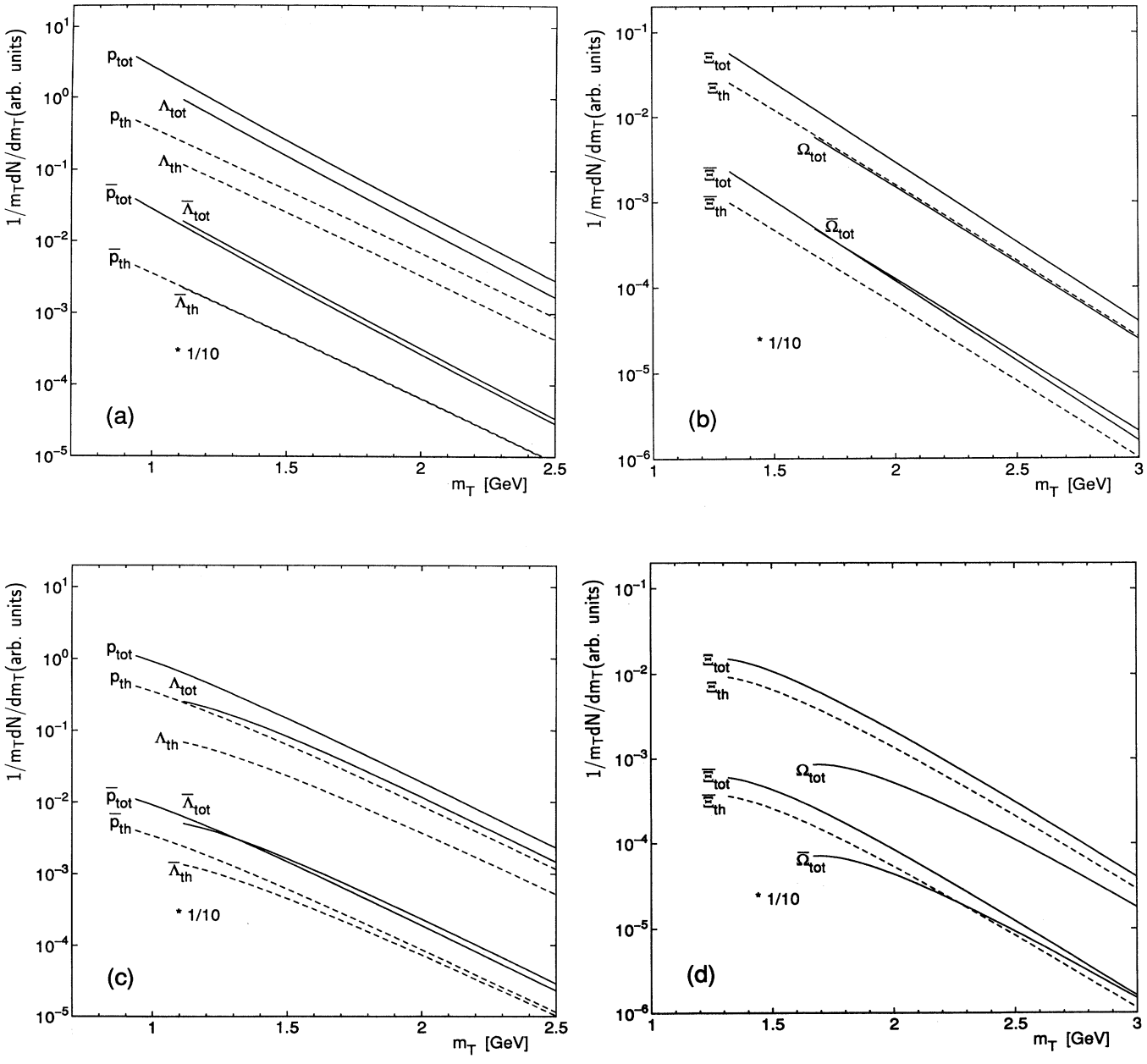

FIG. 3. $m_\perp$ spectra of baryons and antibaryons (yields of antibaryons are shown reduced by a factor 10), arbitrary overall normalization. Spectra in (a) and (b) are for $T = 232$ MeV (no flow) and in (c) and (d) are for $T = 150$ MeV (with flow); for other corresponding parameters see Table I. Dashed lines indicate direct thermal production (subscript "th"); solid lines give total yields including the contributions from resonance decays (subscript "tot").

salt since it may not be easy experimentally to remove the contamination due to projectile and target spectator protons.

In general we regard the ratios predicted in Table II and Fig. 4 as a qualitative test of the idea that the emitter is a fireball which is in thermodynamic equilibrium with the given thermodynamic parameters. It should be kept in mind, however, that even if all predicted ratios should be confirmed experimentally, this will not yet tell us immediately the nature of the emitting source (HG or QGP). To this end we believe that supplementary information concerning the global properties of the source and their *relationship* to the extracted thermodynamic parameters is required, and equally importantly, a study of the systematic behavior of these parameters under varying experimental conditions (collision energy, projectile and target size, collision centrality, etc.). These impor-

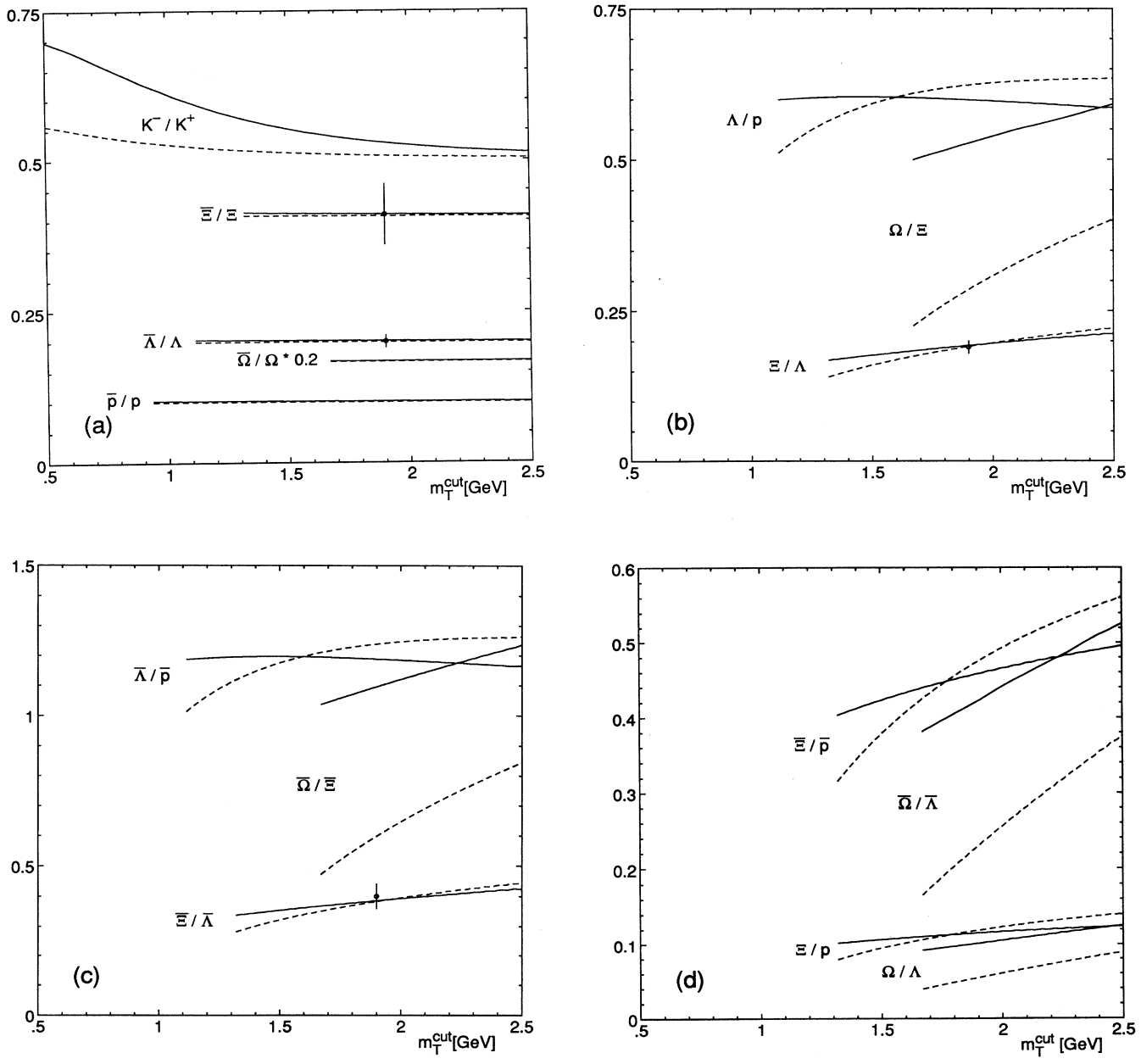

FIG. 4. $m_\perp$-integrated particle ratios as a function of the low-$m_\perp$ cutoff $m_\perp^{\rm cut}$. Solid lines are for $T = 232$ MeV, dashed lines are for $T = 150$ MeV, and the other related model parameters are given in Table I. Different particle ratios are grouped together in (a)–(d). The data points in (a)–(c) correspond to the experimental values to which the model parameters were fitted. In (a) the ratio $\overline{\Omega}/\Omega$ was reduced by a factor of 0.2 to fit into the figure.

tant issues will be discussed in more detail in Secs. IV and V.

4. Relations between strange (anti)baryon yields

There are a number of scenario-dependent and scenario-independent relations between the particle ratios considered. We have already noted some in the preceding discussion. For example, (i) a trivial relationship arising from definitions, e.g., using Eqs. (26) and (27), we see that

$$R_\Lambda \frac{\overline{\Xi}}{\overline{\Lambda}} = R_\Xi \frac{\Xi}{\Lambda}, \tag{56}$$

(ii) a consequence of the finding that the strange quark chemical potential is (nearly) vanishing [see Eq. (28],

$$R_\Lambda \simeq 1.07 R_\Xi^2, \tag{57}$$

$$\overline{\Omega} \simeq \Omega, \tag{58}$$

and (iii) relations arising from cancellation of quark abundances, e.g., (here Λ^t is the direct abundance and it excludes all cascading decays such as $\Sigma^0 \to \Lambda\gamma$),

$$\frac{\Omega^-}{2\Xi^-} \simeq \frac{\Xi^-}{\Lambda^t} \simeq \frac{\Lambda^t}{\mathrm{n}}, \tag{59}$$

and the same for antibaryons; also

$$\frac{\Lambda^t}{p}\frac{\overline{\Lambda^t}}{\bar{p}} \simeq \frac{\Xi^-}{\Lambda^t}\frac{\overline{\Xi^-}}{\overline{\Lambda^t}} \simeq \frac{1}{4}\frac{\Omega^-}{\Xi^-}\frac{\overline{\Omega^-}}{\overline{\Xi^-}} \simeq \gamma_s^2 \tag{60}$$

(relations involving Ω and $\overline{\Omega}$ do not hold well as the omegas do not contain resonance decays).

An interesting question is how sensitive the particle multiplicities are to the constraint arising from the observation of a vanishing strange quark chemical potential and the resulting relationship Eq. (57). In Fig. 5 we show the resulting relation between R_Ξ and R_Λ. The HG results are given for temperatures $T = 200$ MeV (solid line), $T = 150$ MeV (dashed line), and $T = 300$ MeV (short-dashed line), where in each case we insist on strangeness neutrality. The appearance of a finite μ_s impacts the results considerably. For comparison we show (dot-dashed line) results which arise setting $\mu_s = 0$, a natural value for the QGP. The small cross corresponds to the new results reported by the WA85 experiment [6]; the larger cross corresponds to the older data [5]. As can be seen, the $\mu_s = 0$ curve nearly coincides with the $T = 200$ MeV curve and tangents the new data (and old data, as was observed before [20,21]).

We note that the above relations constitute a number of important predictions for the forthcoming Pb-Pb collisions, for which in central interactions we expect $\gamma_s = 1$, in view of the expected longer life span of the high density state. The expected increase in the baryon density of the Pb-Pb fireball will be reflected in an increase in the value of λ_q. This will amplify the anomalies in the strange baryon ratios, raising the relative yields of $\overline{\Omega}$ more than

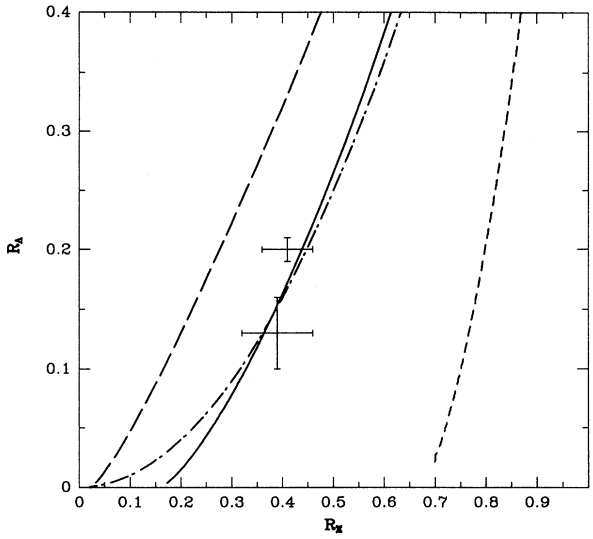

FIG. 5. R_Λ versus R_Ξ. The long-dashed line corresponds to $T = 150$ MeV, the solid line to $T = 200$ MeV, and the dashed line to $T = 300$ MeV in the HG. The dot-dashed line corresponds to $\mu_s \equiv 0$, typical of a QGP. The large cross is the old data [5], the smaller cross more recent results [6] of the experiment WA85.

$\overline{\Xi}$, which in turn increase more than $\overline{\Lambda}$ and finally $\overline{\mathrm{N}}$, provided that again we have $\lambda_s = 1$.

5. High-$m_\perp$ kaon abundances

In addition to the baryon ratios we can also study the ratio of kaons to hyperons, again at fixed $m_\perp$. We have so far not considered this ratio as we are aware of a possible off equilibrium in the relative abundance of mesons and baryons. Thus any deviation seen from the result here obtained should be considered not the failure of the model, but a determination of the relative off-equilibrium abundances of mesons and baryons.

Because of the experimental procedures used, which rely on the observation of the disintegration of neutral strange particles into two charged decay products, a comparison of the K_s^0 with the Λ (which includes the Λ's from the electromagnetic decay of Σ^0's) is the most useful next step. We therefore introduce

$$R_K \equiv \frac{K_s^0}{\Lambda + \Sigma^0} = \frac{1}{8}\frac{\lambda_s/\lambda_d + \lambda_d/\lambda_s}{\lambda_s\lambda_u\lambda_d} \tag{61}$$

where the second identity is only valid if resonance decay contributions cancel. For the rather light kaons there exist many different possibilities for secondary production through resonance decays, which limits somewhat the practical usefulness of this ratio, except at very high $m_\perp^{\mathrm{cut}} > 2$ GeV. However, since the data of the experiment WA85 can be constrained to such large values of $m_\perp^{\mathrm{cut}}$ we show in Fig. 6 the ratio R_K as a function of R_Λ; both ratios are here to be taken as observed at high $m_\perp^{\mathrm{cut}}$. We checked that the effect of resonance cascading indeed

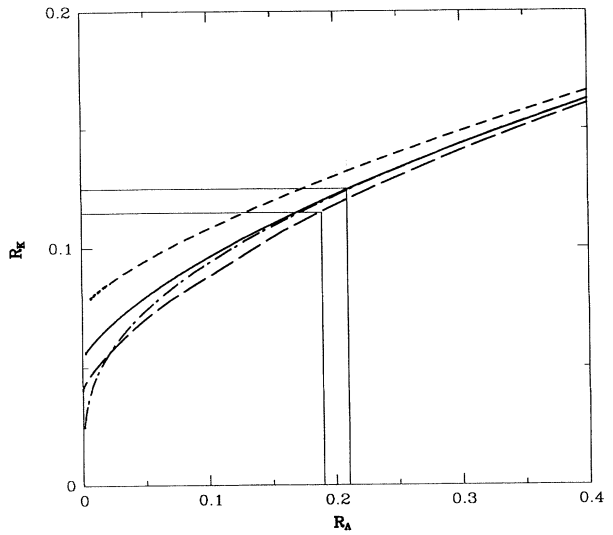

FIG. 6. R_K versus R_Λ with the same conventions as in Fig. 5. The experimental result $0.19 < R_\Lambda < 0.21$ is indicated, as well as the resulting range $0.115 < R_K < 0.125$.

largely cancels in this ratio. The different curves are as in Fig. 5 — the solid line is for $T = 200$ MeV, long-dashed line for $T = 150$ MeV, with strangeness conservation. The dot-dashed line follows for $\lambda_s = 1$, natural for QGP. We also show (short-dashed line) the unrealistically high $T = 300$ MeV, HG result.

Figure 6 shows clearly that the principle of strangeness conservation and the use of the thermal fireball model are sufficient to make a highly precise prediction for R_K once R_Λ is measured. For the observed value $R_\Lambda = 0.20 \pm 0.01$ we expect to obtain $R_K = 0.12 \pm 0.01$. If a significantly different result is found, one might interpret this as an indication for off-equilibrium meson to baryon ratios in the strange sector (see also discussion in Sec. IV).

IV. ENTROPY AND PARTICLE MULTIPLICITY

We have alluded already several times to the fact that while large (multi)strange (anti)baryon abundances indicate the appearance of new physical processes, it is difficult to conclude anything alone on the basis of the current results obtained for one particular collision system at one energy. Other than waiting for the more systematic study of the Pb-Pb system we can only seek to supplement the strange particle multiplicities of the experiment WA85 with complementary data regarding the global particle production and flow [20,22]. Even though for S-W/Pb collisions at 200A GeV no data concerning multiplicity densities in coincidence with strange particle production are yet available, we can consider multiplicity data from a S-Pb emulsion experiment (EMU05 [24]) together with the S-W strangeness production experiment (WA85 [5,6]), both being taken with high multiplicity triggers.

Entropy is the key element in any such discussion, and the entropy content of the reaction is visible through the particle multiplicity. Here we note the relatively high final charged particle multiplicity arising in nuclear collisions: Total charged particle multiplicities (excluding target-projectile fragments) *above* 600 in the central region have been observed by EMU05 [24] in 200A GeV S-Pb collisions, corresponding to a total final particle multiplicity of up to 1000. It is clearly difficult to design an experiment which can simultaneously measure this high particle yield and identify multistrange (anti)baryons. When combining information from the two experiments (EMU05 and WA85) we will also have to remember that the two targets used (^{207}Pb and ^{184}W, respectively) differ in mass by 11% and hence we can expect slightly less stopping of baryon number in the WA85 experiment than in EMU05, resulting very probably in slightly smaller values of baryon density, baryon fugacity, and baryon chemical potential in WA85 compared to EMU05 — as we shall see, this small effect goes in the direction of enlarging the disagreement between the hadronic gas and data; thus, when ignoring it we take the conservative side.

We will argue that in principle the QGP and HG phases are distinguishable in the interesting regime of μ_B, T, γ_s by their entropy content. Since each collision event may have a somewhat different geometry, it is actually more convenient to consider the specific entropy $\mathcal{S}/\mathcal{B}$. It is worthwhile to recall that in a hydrodynamic flow model, in the absence of shock discontinuities, both entropy and baryon numbers are conserved; thus, the time evolution of an isolated fireball occurs at approximately constant specific entropy while the thermal portion of the fireball energy is decreasing due to buildup of the collective flow. We will also develop a relationship between specific entropy and the observable particle flow and discuss a number of possible interpretations of the combined data of WA85 and EMU05.

A. Entropy of a HG fireball

For a fireball consisting of hadronic resonances in thermal and relative chemical equilibrium the entropy content $\mathcal{S}^{\rm HG}$ can be easily computed given the partition function [see Eq. (16)]. The resulting values for the three investigated scenarios are given in Table I. We note that the numbers presented here contain a small correction arising from the nonequilibrium abundance ($\gamma_s \neq 1$):

$$\delta\mathcal{S}^{\rm HG} = \ln\left(\gamma_s^{-1}\right) \sum_{n=1}^{3} n\langle s^n\rangle\,, \tag{62}$$

where $\langle s^n\rangle$ is the number of hadrons with strange and/or antistrange valance quark content number n. Considering how close γ_s is to the equilibrium value it is not surprising that this adds only 0.7 units of entropy per baryon at $\lambda_q \sim 1.5$. This correction is thus small and on the same scale as other uncertainties inherent in our model (like those introduced by the Boltzmann approximation for pions in particular). We will not incorporate these small corrections in the results presented in the fig-

ures, given their qualitative character

For a hypothetical source consisting of a stationary HG at $T_f = 232$ MeV, $\mu_B = 278 \pm 23$ MeV, $\mu_s = 7 \pm 11$ MeV, and $\gamma_s = 0.7$ we obtain from the resonance gas equation of state $\mathcal{S}^{\rm HG}/\mathcal{B} = 18.5 \pm 1.5$. This leads to only about three primary mesons per baryon (before resonance decays), which is not consistent with the high observed total multiplicity. Furthermore, as we have shown, this high T_f is not consistent with the strangeness conservation requirement (it implies a strangeness asymmetry of $\varepsilon = -0.22$). More generally, if we demand strangeness conservation at $\lambda_s = 1$ by appropriately adjusting the temperature as a function of μ_q, we obtain a unique relationship between $\mathcal{S}/\mathcal{B}$ and λ_q. This is shown in Fig. 7 by the thin solid line (with $R_f = 1.08$ appropriate for S-W, S-Pb collisions). The value at $\lambda_q = 1.48$ MeV corresponds to the thermal parameters for the case (C) in Table I ($T_f = 190$ MeV, $\mu_B = 223 \pm 19$ MeV); at $\lambda_s = 1$, $\gamma_s = 0.7$, we have a specific entropy content of 25 units. This is the only point in the equilibrium hadronic gas consistent with the notion of strangeness conservation (for discussion of dashed, dotted, and thick lines, see Secs. IV C 1 and IV C 2). A considerable increase in specific entropy ensues when we consider the freeze-out temperature $T_f = 150$ MeV (for the reasons given before). While such a HG source would be sufficiently rich in entropy to be consistent with the high particle multiplicities seen by EMU05 experiment (see below), strangeness neutrality would require $\lambda_s \sim 1.2$, nearly 4 s.d. outside the limits established by our data analysis. At $\lambda_s = 1.03$ (see Table I), we find a net strangeness asymmetry $\varepsilon = 0.37$. Furthermore, this state has also a thermal energy per baryon of $\mathcal{E}/\mathcal{B} = 8$ GeV, which is 85% of the available center-of-mass energy in the experiment and in strong contradiction with the evidence for incomplete stopping and partial transparency from the particle rapidity spectra. We conclude that this way to enhance multiplicity (low T only) is fraught with insurmountable difficulties.

B. Particle multiplicity and charge flow

The above remarks about an insufficient entropy content of the HG model can be made more quantitative by relating them to the observed charged particle production. A very useful quantity is the ratio of the net charge to the total charged multiplicity [22]:

$$D_Q \equiv \frac{N^+ - N^-}{N^+ + N^-} \,. \tag{63}$$

Within the HG model the value of D_Q can be calculated for any set of thermal parameters. To this end the resonance decays have to be decomposed into their various isospin channels. In particular the decay of neutral mesons into charged particle pairs impacts the value of D_Q significantly. To illustrate this we also computed the value D_Q^0 at freeze-out before the decay of resonances. In Fig. 8 we show the relationship between D_Q^0, D_Q, and μ_B, again assuming $\lambda_s = 1$ and strangeness conservation — the upper curves are for D_Q^0, the lower curves include decays, and we have indicated the range of the uncertainty in $\lambda_s = 1 \pm 0.05$; the dotted line is $\lambda_s = 1.05$, and the dashed line is $\lambda_s = 0.95$. The decay of neutral resonances raises the charged particle multiplicity and reduces at given μ_B (and hence T) the observed value of D_Q. Because of the complexity of the calculation, the simplicity of this result is surprising. From Fig. 8 we

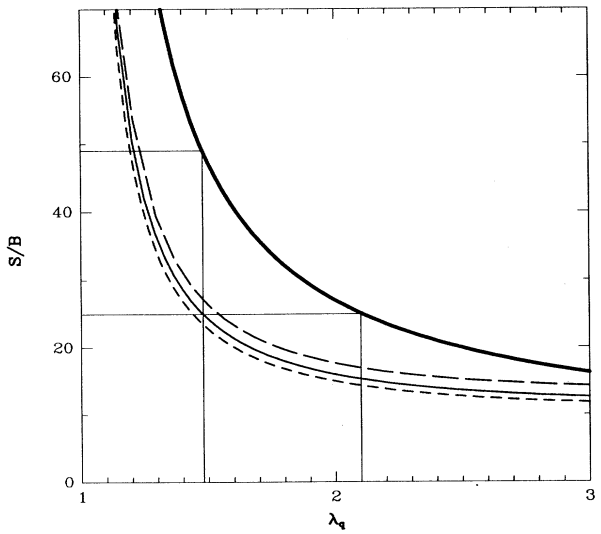

FIG. 7. Specific entropy $\mathcal{S}/\mathcal{B}$ as function of quark fugacity λ_q for the HG phase with $\lambda_s = 1$ (as fixed by experiment) and with T fixed by the strangeness neutrality condition, Eq. (23) (thin solid line), Eq. (71) (dashed line for $R_C = 1.5$ and long-dashed line for $R_C^s = 0.39$). Thick solid line: QGP. Horizontal and vertical lines guide the eye.

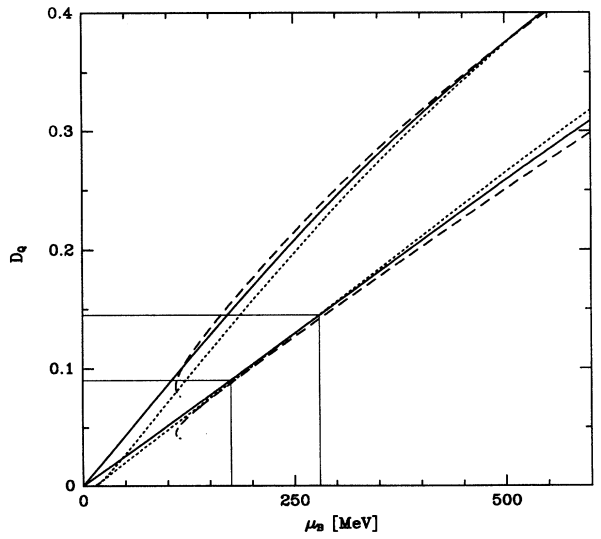

FIG. 8. D_Q^0 (upper curves) and D_Q as a function of μ_B for fixed $\lambda_s = 1 \pm 0.05$ and conserved zero strangeness in a HG. The error in λ_s is bracketed by dotted and dashed curves: dotted for $\lambda_s = 1.05$, dashed for $\lambda_s = 0.95$. Horizontal and vertical lines guide the eye.

obtain, approximately,[6]

$$D_Q^0 \approx \frac{\mu_B}{1.2\ \text{GeV}} \quad \text{for} \quad \mu_B < 0.3\ \text{GeV}, \tag{64}$$

$$D_Q \approx \frac{\mu_B}{1.95\ \text{GeV}} \quad \text{for} \quad \mu_B < 0.6\ \text{GeV}. \tag{65}$$

The horizontal and vertical lines guide the eye to show that the experimentally observed values of D_Q and μ_B are not consistent with each other. We will return to this question further below.

1. Relation between $\mathcal{S}/\mathcal{B}$ and D_Q

The variable D_Q represents essentially the inverse of the specific entropy. To see this we note that the quantity $D_Q^0(\mathcal{S}/\mathcal{B})$ is effectively a measure of the entropy per pion. Very qualitatively we have (in the absence of strange particles, neglecting the small u-d asymmetry, and assuming pion symmetry $N_{\pi^+} = N_{\pi^-} = N_{\pi^0} = N_\pi/3$)

$$D_Q^0 \to 0.75 \frac{\mathcal{B}}{N_\pi} \frac{1}{1 + 1.5 \sum_i N_i/N_\pi}, \tag{66}$$

where the last term in the denominator involves the sum over all initial charged particles other than pions, in particular heavy mesons, protons, antiprotons, etc. In the product D_Q^0 with $\mathcal{S}/\mathcal{B}$ the baryon content cancels, and the result is roughly the entropy per pion. Consequently we expect the result to depend only weakly on the thermal parameters. This is confirmed by Fig. 9 where we show the product $D_Q\mathcal{S}/\mathcal{B}$ at $\gamma_s = 0.7$, as a function of λ_q for fixed $\lambda_s = 1 \pm 0.05$, with T adjusted at each value of λ_q to ensure strangeness neutrality. The lower set of curves includes resonance decays whereas the upper set is for D_Q^0. We observe that within the here interesting range of parameters these curves are pretty flat, and the strangeness neutral equilibrium HG fireball, allowing for cascading and decays, satisfies the relation

$$(\mathcal{S}/\mathcal{B}) D_Q \simeq 3.0 \pm 0.2 \tag{67}$$

determining the entropy content in terms of the normalized charge asymmetry. We note in Fig. 9 the lack of sensitivity of the result to the presence of strange particles: The dot-dashed curves show results obtained with a very small fraction of strangeness being present, but with temperature T still constrained by the requirement that for each value of λ_q we have strangeness conservation at $\lambda_s = 1$.

Finally we consider in Fig. 10 the relationship between the specific entropy $\mathcal{S}/\mathcal{B}$ and D_Q^{-1} at $\lambda_s = 1$, by eliminating the remaining thermal parameter (λ_q or equivalently μ_B). The solid upper curve is the result without decays (note that for this case the horizontal axis corresponds to $1/D_Q^0$). The dot-dashed line gives the result in the absence of strange particles (e.g., for $\gamma_s \to 0$). We note that

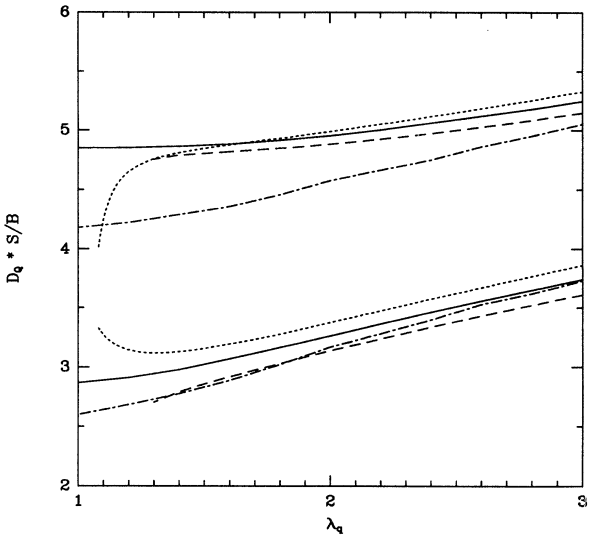

FIG. 9. The product $D_Q^0(\mathcal{S}/\mathcal{B})$ (upper curves) and $D_Q(\mathcal{S}/\mathcal{B})$ (lower curves) as a function of λ_q for fixed $\lambda_s = 1 \pm 0.05$ (compare to Fig. 8). The dot-dashed curves were obtained with negligible strange particle content ($\gamma_s \to 0$). Note the suppressed zero on the vertical axis.

the strange flavor content plays a rather minor role in establishing the relation between $\mathcal{S}^{\text{HG}}/\mathcal{B}$ and D_Q^{-1}, which indicates that both strange and nonstrange particles separately satisfy similar functional relationships. For a discussion of the long-dashed and short-dashed curves see Sec. IV C 2; the vertical lines guide the eye regarding the

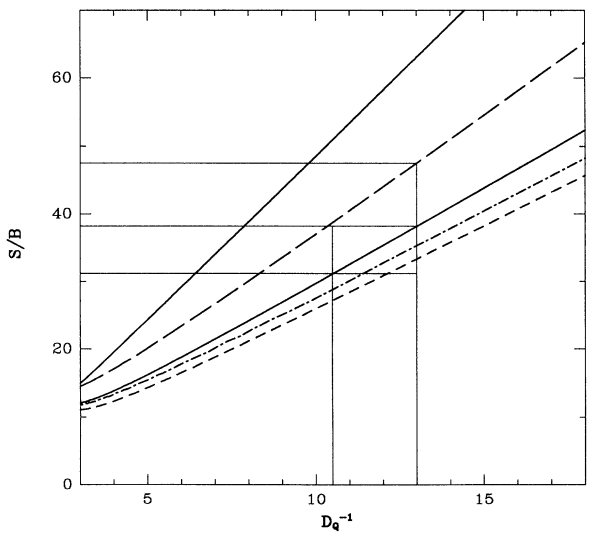

FIG. 10. Entropy per baryon $\mathcal{S}/\mathcal{B}$ as a function of D_Q^{-1} for fixed $\lambda_s = 1$ and conserved zero strangeness. Only the one upper solid line curve corresponds to D_Q^0 (prior to strong decays of hadronic resonances); all others include resonance decay. The solid lines are both for $R_C = 1$. The long-dashed curve corresponds to $R_C = 0.39$, the lower dashed curve to $R_C = 1.5$, and the dot-dashed curve shows the limit $\gamma_s \to 0$ (negligible strange particle content).

[6]The result for D_Q^0 is slightly different from [22] due to improvement of the equation of state to include twice as many hadronic resonances.

range of experimental values for D_Q, (see below); the horizontal lines indicate the resulting values of specific entropy.

2. Comparison with emulsion data

The EMU05 Collaboration has made available to us some of their unpublished data [24] on charged multiplicity as a function of pseudorapidity. They are shown in Fig. 11. In order to be independent of the bias introduced by the high multiplicity trigger, we only consider the particle ratio D_Q as a function of (pseudo)rapidity. The data points correspond to 15 fully scanned "central" events of 200A GeV S-Pb interactions, with the trigger requirement being a total charged multiplicity > 300. Reaction spectators (target fragments) are not observed in this experiment. At central rapidity a value of 0.08–0.09 is found for D_Q. The smallest values of D_Q correspond to a peak in the total charged multiplicity distribution combined with a slight dip in the net charge distribution near central rapidity [24]. We also note the rise of D_Q in the projectile and target pseudorapidity regions, caused by a faster decrease in the fragmentation regions of the total particle multiplicity (mostly pions) than of the positive particle excess (protons). Obviously these features display the partial transparency at CERN energies of the Pb nucleus to the incoming sulphur projectile; it will be interesting to see whether this behavior of D_Q persists for heavier projectiles, and in particular how the shape $D_Q(y)$ changes for Pb-Pb collisions.

We note that the measured very small central values of D_Q imply a relatively large value for $\mathcal{S}/\mathcal{B}$. Taking the *experimental* value $D_Q = 0.085 \pm 0.01$ we find from Fig. 10 (see vertical lines there) and Eq. (67) that the specific entropy of the source ought to be $35^{+5}_{-2.5}$. In order to obtain the values of entropy characteristic of the strangeness neutral HG, with thermal parameters extracted from the strange particle multiplicities and spectra, we need $D_Q \simeq 0.12 - 0.13$ which is about 4 s.d. away from the EMU05 data; see Fig. 11. We have thus not succeeded in the task of developing a HG-based model which could yield the observed $D_Q \simeq 0.08$ when $\lambda_q = 1.48$ and $\lambda_s \simeq 1$ with strangeness neutrality being satisfied.

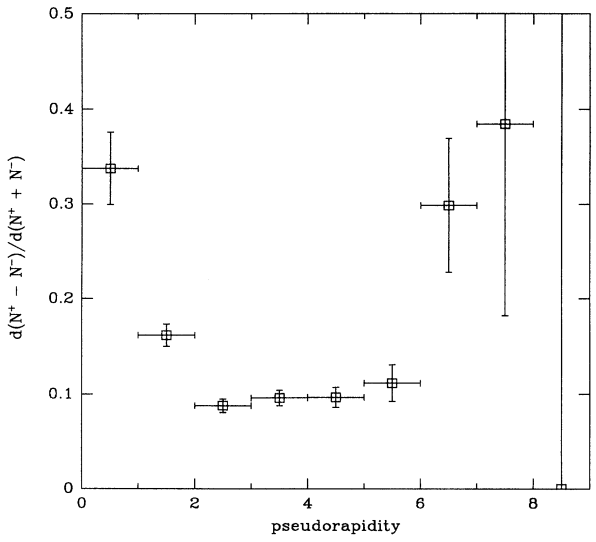

FIG. 11. Emulsion data for the charged particle multiplicity from central S-Pb collisions at 200A GeV as a function of pseudorapidity: the difference of positively and negatively charged particles normalized by the sum of both polarities. (Courtesy of CERN-EMU05 collaboration, Y. Takahashi *et al.* [24].)

We conclude that none of the equilibrium HG freeze-out models listed in Table I can describe all data and/or is logically satisfactory. As described this is not primarily due to a failure of the thermal picture and/or the fireball model, but is caused by the impossibility of satisfying all of the strict constraints imposed by the assumption of a HG equation of state. For example, as just seen this EOS is not able to provide sufficient particle multiplicity (and thus entropy) to yield agreement with the multiplicity data. The principle of strangeness neutrality has further constrained us to a freeze-out temperature $T = 190$ MeV which is incompatible with our general knowledge of hadronic interactions. In the remainder of the paper we will therefore feel free to embark on more speculative studies of the nature of the thermal fireball in order to assess the chances for possible alternative explanations of the data.

C. Entropy content and hadronization of a quark-gluon plasma

The major reason to think about the QGP phase as an alternative for the structure of the fireball is the appearance in all experiments done at 200A GeV of a large degree of strangeness saturation ($\gamma_s \to 1$), accompanied by a practically vanishing strange quark chemical potential. We believe that in a QGP phase strangeness equilibration occurs relatively fast, and the value $\mu_s = 0$ is a natural consequence of strangeness neutrality at any T and μ_B. This implies in particular that $\mu_s = 0$ is also compatible with a low freeze-out temperature of 150 MeV or even less (accompanied by a correspondingly large transverse flow), which would bring the freeze-out picture into agreement with lattice QCD estimates of the hadronization temperature. Thus a hadronizing QGP phase has some attractiveness worth to be explored as an alternative to the HG model which we found to be in discrepancy with the data.

1. Specific entropy of the QGP phase

The specific entropy of a quark-gluon plasma can be estimated from the perturbative QGP equation of state. Up to corrections of order $(\mu_q/\pi T)^2 \sim 0.02$, the leading term of the specific entropy from light quarks and gluons is

$$\frac{\mathcal{S}^{\mathrm{QGP}}}{\mathcal{B}} = \frac{3\pi^2}{2}\left(\frac{T}{\mu_q}\right)\left[\frac{14(1-50\alpha_s/21\pi)}{15(1-2\alpha_s/\pi)} + \frac{32(1-15\alpha_s/4\pi)}{45(1-2\alpha_s/\pi)}\right] = 17\,(T/\mu_q) = \frac{17}{\ln\lambda_q} \quad \text{for } \alpha_s = 0.6\,. \tag{68}$$

We see that the specific entropy from light quarks and gluons depends only on the ratio μ_q/T, and that isentropic expansion (at $\mathcal{S}^{\rm QGP}/\mathcal{B}=$ const) of an equilibrated QGP occurs at constant λ_q. To the extent that the measured value of λ_q reflects its value in the early QGP phase (see Sec. IV C 2), the specific entropy of that phase is thus independent of the specific combination between freeze-out temperature and transverse flow reflected in the slope of the $m_\perp$ spectra. At the extracted value $\lambda_q = 1.48 \pm 0.05$ already the nonstrange fraction of the QGP contributes 43 ± 4 entropy units per baryon. We must add to this result also the entropy content of the strange quarks in the plasma, which have no net baryon number. In principle this contribution does depend slightly on the temperature, due to the nonvanishing strange quark mass, for the here relevant regime of $T > m_s \simeq 150$ MeV; however, this temperature dependence can be ignored. For the same reason we can argue that perturbative QCD corrections are of the same magnitude as for light quarks considered before and hence the entropy content of hadronizing QGP is as if there were not two, but three quark flavors. We thus obtain, instead of Eq. (68),

$$\frac{\mathcal{S}^{\rm QGP}}{\mathcal{B}} = \frac{19}{\ln \lambda_q} \quad \text{for } \alpha_s = 0.6 \tag{69}$$

which is shown as the thick solid line in Fig. 7. We thus expect the QGP to possess in total about 50 ± 10 units of entropy per baryon at the given value of $\lambda_q = 1.48$ (see long vertical line in Fig. 7), where the error estimate includes the uncertainty in the value of α_s and of the strange quark mass and its influence on the α_s corrections.

To understand better the difference between QGP and HG models we consider under which conditions a QGP would have a similarly low specific entropy ($\simeq 25$) as the (equilibrium) HG considered above. We find that a value $\lambda_q = 2.1$ (see short vertical line in Fig. 7) would yield about the right answer — this would imply quite different particle ratios than those measured (which correspond to $\lambda_q = 1.48 \pm 0.05$). On the other hand, we cannot obtain such large specific entropy in a HG phase at the given value of λ_q, respecting $\lambda_s = 1$ and strangeness conservation. If $\lambda_s = 1$ is forsaken, then the temperature to be considered is as low as $T \sim 135$ MeV (which requires $\beta_f \sim 0.5$); at this temperature strangeness neutrality leads to $\lambda_s \simeq 1.3$ which is far outside the observed parameter range ($\lambda_s = 1.03 \pm 0.05$). Thus it appears that the specific entropy content of the final state should easily distinguish between the two extreme phases of the fireball.

2. *Meson-baryon nonequilibrium*

In our consideration of strangeness conservation we have implicitly assumed that the ratio of strange mesons to baryons is the same as found in full equilibrium. Similarly, in our discussion of the relationship of D_Q with μ_q and specific entropy $\mathcal{S}/\mathcal{B}$ the important implicit assumption was the presence of a relative meson-baryon abundance equilibrium. Are these assumptions justified when we consider the QGP as source of the diverse particles? We should think so only if hadronization is a slow process. However, the motivation to study the QGP came from observations which require a rapidly hadronizing QGP phase such that it is possible to preserve the chemical potentials which parametrize the relative abundances of the various quark flavors and would then lead to corresponding relative abundances of the hadrons. For previous discussions of a rapid QGP breakup with statistical quark recombination we refer to [3,19,41–43]. Since the internal phase space of three quarks inside a baryon is different from that of a quark-antiquark pair in a meson, we should expect an overall difference between baryon and meson coalescence rates in the recombination process [3]. Thus while relative chemical equilibrium among baryons and among mesons may be preserved separately by the hadronization process the overall meson/baryon ratio need not follow the laws of relative chemical equilibrium. Subsequent hadronic processes are not likely to reestablish meson-baryon equilibrium: It takes a three-body reaction to absorb a meson, and it takes a rare collision such as $\rho+\omega \to N+\overline{N}$ at sufficiently high $\sqrt{s}$ to produce a baryon-antibaryon pair. At sufficiently low hadronization temperatures these processes are suppressed. We must also require that most particles be produced at low enough temperature for the emerging hadron system to be sufficiently dilute for immediate (chemical) decoupling of the abundances. Inelastic hadronic final state interactions would tend to change these relative abundances in the direction of HG equilibrium (with generally $\mu_s \neq 0$) and should have a sufficiently slow rate to be negligible until thermal decoupling.

We thus expect that the hadronic gas which will emerge from the QGP hadronization will have particle abundances which are largely off equilibrium and a direct comparison of meson and baryon abundances is not easily possible. We have made a number of studies in order to assess the remaining predictive power of our approach in such more complex circumstances. While a complete discussion goes beyond the scope of this paper we can explore briefly a minimal model in which globally the abundances of mesons and baryons are multiplicatively changed compared to the chemical abundance expectations. All quantities depend only on the ratio of the off-equilibrium factors for mesons C_M and for baryons C_B:

$$R_C = \frac{C_M}{C_B}, \tag{70}$$

with the exception of the final state D_Q which can be affected by differing numbers of mesons available to the decay. Note that in general the nonequilibrium abundance factors drop out from baryon/(anti)baryon and meson/meson (but not from baryon/meson) ratios — in particular, λ_q and λ_s can still be extracted from the strange (anti)baryon ratios as before, with the same outcome.

In the strange particle sector the effect of R_C is unexpectedly large; the strangeness conservation condition at $\lambda_s = 1$, Eq. (23), now takes the form

$$\mu_B^0 = 3T \operatorname{arccosh}\left(R_C \frac{F_K}{2F_Y} - \gamma_s \frac{F_\Xi}{F_Y}\right). \quad (71)$$

Even for the relatively modest range $0.39 < R_C < 1.5$ one finds a wide range of T-μ_B parameters which allow strangeness conservation. In Fig. 12 we show the strangeness conservation constraint (for $\lambda_s = 1$) with $R_C = 1$ (solid line), $R_C = 0.39$ (long-dashed line), and $R_C = 1.5$ (short-dashed line). The hatched area indicates the values of μ_B and T compatible with the chemical abundances fixed by the WA85 data, with the scale of temperature gauged by the transverse mass spectra — the cross corresponds to the value of $T = 232 \pm 5$ MeV (no flow) where $R_C = 1.5$ in order to satisfy strangeness neutrality condition; for $T = 190$ MeV we need $R_C = 1$, and for $T = 150$ MeV, $R_C = 0.39$. There is also considerable impact of R_C on the relation between $\mathcal{S}/\mathcal{B}$ and D_Q^{-1} shown in Fig. 10; the long-dashed curve corresponds again to $R_C = 0.39$ and the short-dashed curve to $R_C = 1.5$ (in both cases C_M, which was the same for strange and nonstrange particles, was changed, and $C_B = 1$; for $C_M \to 0$ the long-dashed line and the upper solid line nearly coincide since there is no meson disintegration impacting D_Q).

We see in Fig. 10 that the values of D_Q^{-1} which correspond to the central rapidity result of EMU05 [24] (see Fig. 11, bracketed by the vertical lines) correspond to $\mathcal{S}/\mathcal{B} \sim 40$–$48$, which is nearly consistent with a hadronizing QGP state. However, we note that this range of values of D_Q would be attained at $\lambda_q \sim 1.3$ as shown in Fig. 13, where we display the relation between D_Q and λ_q for a strangeness neutral system at $\lambda_s = 1$. The experimental data point is based on the direct EMU05 observation [24] of D_Q and our interpretation in Eq. (32) of the WA85 data [6] in order to obtain λ_q. The upper curves which show D_Q^0 before resonance decays miss the measured value by EMU05 by more than a factor 2 [22]; the lower three curves show D_Q after resonance decays— again the long-dashed curves correspond to $R_C = 1.5$ and short-dashed curves to $R_C = 0.39$ (recall that we kept $C_B = 1$ and hence the changes in D_Q with R_C reflect changes in C_M). The disagreement with EMU05 is smaller after resonance decays, in particular for values $R_C > 1$, which, however, imply unreasonably high temperatures of hadronization (see Fig. 12) — each point on every curve is characterized by a definite temperature at which the strangeness neutrality is satisfied with the given λ_q. We see that for the preferred lower freeze-out temperatures ($T = 150$ MeV, $R_C = 0.39$) the disagreement with the EMU05 data gets actually worse when we have just one hadronization parameter which is adjusted to ensure strangeness neutrality. The effect amounts to about three standard deviations, and in our opinion necessitates introduction of a second (or more) QGP hadronization parameter(s).

This point is also noted considering two other results: Introducing just one off-equilibrium parameter R_C we have found that the results presented in Fig. 6 where we compare strange mesons and baryons are not much affected. Similarly, there is little impact of R_C on $\mathcal{S}/\mathcal{B}$: In Fig. 7 we show by a dashed line the specific entropy relation with λ_q for $R_C = 1.5$ and the long-dashed line is the case $R_C = 0.39$. Despite this relative wide range of parameters we see little impact, as the curves have for each λ_q a different value of temperature at which the strangeness neutrality is reached: $T = 232$ (150) MeV for

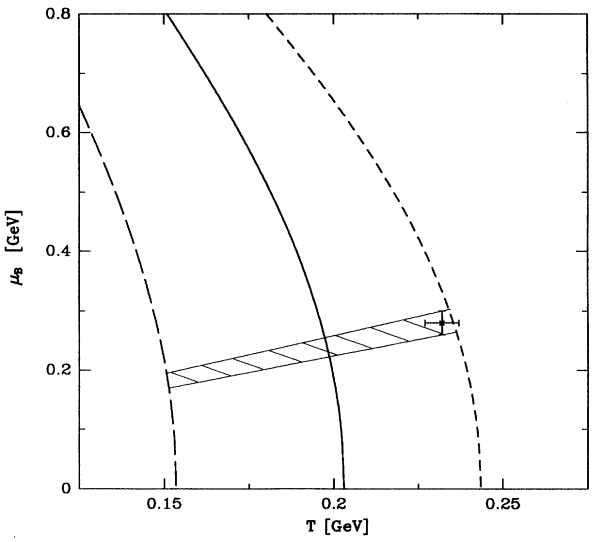

FIG. 12. Strangeness conservation constraint in the μ_B-T plane for $\lambda_s = 1$ with $R_C^s = 1$ (solid line), $R_C = 1.5$ (dashed line), and $R_C = 0.39$ (long-dashed line). The hatched area indicates the values of μ_B and T compatible with the relative particle abundances and transverse mass spectra; the cross corresponds to the experimental values without flow.

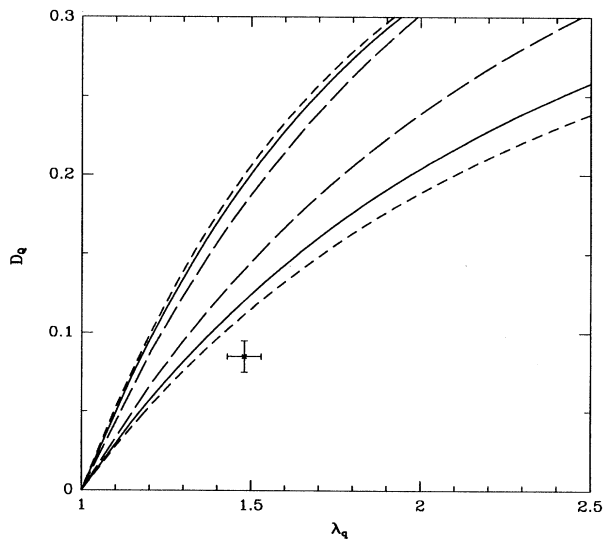

FIG. 13. Lower three curves: $D_Q(\lambda_q)$ at $\lambda_s = 1$. Upper three curves: same before decays (D_Q^0). $R_C = 1$ (solid lines), 1.5 (dashed lines), and 0.39 (long-dotted lines) for strangeness-neutral systems. The experimental point is based on EMU05 [24] data for D_Q and our interpretation [see Eq. (32)] of WA85 data [6].

$R_C = 1.5$ (0.39). This finding, viz., that the relation of entropy to λ_q is little dependent on R_C, clearly indicates that in a hadronizing entropy-rich QGP there must at least be two nonequilibrium parameters in order to allow for the transfer of the high entropy to the final hadronic state. Note that in principle the off-equilibrium factors for strange and nonstrange particles are independent of each other,

$$C^s_{M,B} \neq C_{M,B}\,, \tag{72}$$

and hence there are at least two additional parameters (e.g., R_C and R^s_C) in a model of this character. We believe that it is possible to obtain a satisfactory description of all currently available data in such an approach, since we could change independently the ratio of pions to baryons and in that way explain the high entropy and particle multiplicity observed, while R^s_C provides for a suitable change in the constraint between λ_q and λ_s.

We conclude that in a phenomenological description of hadronizing QGP phase the breaking of the meson/baryon thermal equilibrium ratio in the final hadronic state by the single parameter is not sufficient to save simultaneously the strangeness neutrality and enhance entropy balance during hadronization of a QGP. More complicated changes in particle abundances, which in particular decouple the strange from nonstrange particle abundances, are needed in order to describe the full set of current data. A valid description, involving a QGP, must await development of detailed QGP hadronization models in order to reduce the large number of possible parameters to be considered. However, it should not be believed that the introduction of a large number of parameters will automatically yield a good description of the experiments — the constraints between the observables and conservation laws are very strong and not easily satisfied, as we have experienced in this qualitative first exploration.

V. CONCLUSIONS

Our present work was primarily oriented towards an in-depth thermal and chemical analysis of the S-W and S-Pb results obtained by the WA85 [5,6] and EMU05 [24] Collaborations at the CERN SPS with $200A$ GeV/c beams. Within a thermal model we have extracted, from the nuclear collision data, the characteristic statistical properties of the particle-emitting source. Our analysis relies strongly on the (at least approximate) validity of the concepts of thermal and relative chemical equilibrium. We have provided predictions which allow one to test these ideas. In the following discussion we will summarize the implications for conceivable nuclear collision scenarios, in particular regarding the evolution and freeze-out (breakup) of the fireball into the final state hadrons.

We first address the stunning result $\lambda_s = 1$, which acquires particular importance if it is combined with the constraints arising from strangeness conservation. We have considered the possibility that the appearance of this value for λ_s could be an accident of usual hadronic reaction dynamics, especially if one initially disregards entropy considerations. For this to work the observed apparent temperature $T_{\rm app} = 232 \pm 5$ MeV has to be taken as just the right mixture of the true freeze-out temperature $T_{\rm f} = 190$ MeV and a collective transverse flow $\beta_f = 0.2$ — only under these conditions can the requirement of strangeness neutrality be satisfied with a hadron gas picture. Aside from the clearly accidental nature of such an explanation we note the difficulties in justifying such high freeze-out temperatures.

This seemingly accidental appearance of $\lambda_s = 1$ repeats itself [25] in S-S collisions at $200A$ GeV, but not at the lower AGS energies of $15A$ GeV. There one finds $\lambda_s \sim 1.7$ [29], which is entirely consistent with strangeness conservation in a HG at the corresponding value $\lambda_q \sim 3.7$. This conventional result obtained at low energies amplifies the importance of the result $\lambda_s = 1$ obtained at $200A$ GeV, since this is a natural value in all forms of hadronic matter in which strangeness is not bound inside baryons or baryonlike clusters — in the latter case the finite baryon density breaks the strange particle-antiparticle symmetry.

While the appearance of $\lambda_s = 1$ is in itself strongly suggestive of novel physics, it is even harder to explain the large degree of strangeness saturation, $\gamma_s \simeq 0.7$. The corresponding value in N-N collisions is known to be much lower ($\gamma_s = 0.2$ [25]), and estimates of the usual hadronic equilibration time scales [2] suggest that there is not nearly enough time to raise it to the observed value during a nuclear collision. In particular the implicit assumption $\gamma_s = 1$ in complete chemical equilibrium HG scenarios [21,23]) cannot be justified. We find it significant that the new higher precision data from WA85 [6] indeed exclude the possibility of a fully equilibrated HG with $\gamma_s = 1$. A thermal explanation of these data clearly requires the option of *nonequilibrium strange particle abundances.*

Of course, once this has been established, the question arises whether the introduction of the single parameter γ_s is sufficient to describe the observed deviations, or whether the deviations from chemical equilibrium are more complex, perhaps indeed to the extent that the concept of (even the less demanding relative) chemical equilibrium becomes useless. Our introduction of the parameter γ_s was motivated by the intuitive idea based on kinetic arguments that the dominant deviations from equilibrium should be due to an overall under saturation of the strange sector. This particular way of generalizing the thermal model still allows one to keep some order in the chemical nonequilibrium structure, thus salvaging most of the attractive simplicity of thermal models. As shown it permits us to explain the WA85 (multi)strange (anti)baryon data in a systematic way using the concept of *relative chemical equilibrium* in the strange sector, and provides predictions for further particle ratios.

However, in addition to the problems with strangeness neutrality in this approach which requires one to assume an inconsistently high freeze-out temperature, we found a problem of this interpretation with the net and total charged multiplicity data of EMU05 [24]. If inter-

preted within this model these data indicate the presence of a larger specific entropy than compatible with the extracted thermal parameters. This manifests itself in the observation $D_Q = 0.085$ at central rapidity, instead of the value 0.12 expected from the model — this translates into a 40% higher charged multiplicity pseudorapidity density per participant baryon than provided by the HG model. A very similar result is found in an analysis of global (4π) particle production data from S-S collisions [25]. This implies that there are further deviations from chemical equilibrium in the final hadron gas state residing in those particle species not observed or properly identified by WA85 [5,6] and NA35 [7], which are responsible for the excess specific entropy.

Looking for a possible origin of the high specific entropy in the final state, which at the same time explains the vanishing of the strange quark chemical potential and the high degree of strangeness saturation, we also studied the thermodynamic properties and hadronization of a deconfined quark-gluon plasma phase. If the observed chemical potentials of the final hadrons are indicative of the chemical conditions of this QGP phase (which, as we pointed out, requires rapid hadronization followed by immediate decoupling), the specific entropy is nearly 100% larger than that of the generalized HG with the same parameters. This might indicate QGP formation in a fraction of the fireball volume or of the nuclear collision events at the SPS energy of 200A GeV, promising larger fractions and larger values of $\mathcal{S}/\mathcal{B}$ and γ_s in the upcoming Pb-Pb experiments.

Following this line of thought we then discussed possible QGP hadronization scenarios which would be compatible with the experimental observations. A sudden transition is required to preserve the chemical potentials, in particular the vanishing strange quark chemical potential. Immediate (chemical) decoupling after hadronization would guarantee the preservation of these values until thermal freeze-out, indicating the need for a sufficiently low freeze-out temperature. This would also bring the model in line with recent QCD lattice calculations [27] which predict a transition temperature of about 150 MeV and would imply the existence of a strong flow component in the $m_\perp$ spectra as previously suggested on the basis of kinetic freeze-out arguments. This picture also suggests a particular mechanism for an additional breaking of chemical equilibrium in the final hadron state which (as we saw above) is required by the entropy discrepancy: We propose that QGP hadronization breaks in a natural way the relative chemical equilibrium between mesons and baryons. The condition of immediate chemical decoupling already required by the preservation of μ_s would also guarantee the survival of this new nonequilibrium feature until thermal freeze-out.

We have parametrized this effect by the ratio R_C of relative meson to baryon coalescence probabilities. We found that the introduction of this parameter makes it easy to reconcile low freeze-out temperatures with the strangeness neutrality condition, but that we cannot easily satisfy the entropy balance. The development of a consistent hadronization scenario which also solves this crucial remaining problem remains a challenge for the future.

Others have tried in various ways to salvage the equilibrium HG picture. In this paragraph we would like to take issue with one such approach, thereby further emphasizing the crucial difficulties faced by any thermal interpretation of the presently available nuclear particle production data. It was postulated in [23] that strange and nonstrange hadrons freeze out at different temperatures and different values of μ_B. The nonstrange hadrons are assumed to decouple at $T \simeq 130$ MeV with a sufficiently low value of μ_B to reproduce the large specific entropy, while the strange particles are supposed to escape already at $T = 210$ MeV (as indicated by the old data [5,36]), with values of μ_B and μ_s consistent with our analysis. Since with these parameters the conventional hadron resonance gas yields only 70% of the measured specific entropy, and it is unlikely that the missing entropy can be created in the hydrodynamic expansion process while cooling from $T = 210$ MeV to $T = 130$ MeV, it is postulated that at the earlier stage of strange particle freeze-out the HG is in an "exotic," very strongly interacting, state whose specific entropy is by about a factor of 1.4 larger than usual. However, under such circumstances one has to expect strong medium modifications of the properties of *all* hadrons (including the strange ones), and it is no longer consistent to use the smaller free-space cross sections of strange hadrons as an argument for their earlier freeze-out [23]. Furthermore, this picture of sequential freeze-out at two quite different temperatures does not automatically yield the observed similar $m_\perp$ slopes of all hadrons, and a detailed study of the amount of flow generated in the time interval between strange and nonstrange particle freeze-out has not been performed. Finally, the analysis in [23] of the nonstrange hadrons by a HG at $T = 130$ MeV does not take into account the considerable loss of energy, entropy, and baryon number by the earlier freeze-out of the strange hadrons, and hadrons with hidden strangeness like the ϕ are treated like nonstrange hadrons, although their cross sections are also small and should cause them to freeze out early together with the other strange particles. These severe consistency problems imply in our opinion that the sequential HG freeze-out scheme of Ref. [23] does not provide a valid framework for an explanation of the data. (Also, the new WA85 data [6] appear to cause further difficulties for this model.)

We see that the freeze-out criterium turns out to be a severe constraint on all thermal models. Together with the particle abundances and their characteristic deviations from chemical equilibrium we hope that eventually enough information becomes available to permit construction of a fully dynamical hadronization scenario. Present data show an intriguing compatibility with the ideas of thermal and chemical equilibrium in certain particle sectors, but at the same time a characteristic failure of these concepts in others. It is necessary to widen the investigation of strange meson and (anti)baryon ratios to higher *and* lower nuclear beam energies and to study simultaneously the particle multiplicity and charge flow at high and low $m_\perp$, in order to eliminate the remaining freedom in the models. We are therefore looking forward

with anticipation to the forthcoming Pb-Pb collisions at about 170A GeV projectile energy, which will allow us to check and extend the results of our analysis by going to the largest possible thermodynamic systems using nuclear collisions. For the time being, we have shown that the interpretation of the S-W, S-Pb data in terms of a thermal model implies a primordial state, which is not a conventional HG phase.

Note added in proof

Since the revised version of this paper was submitted, new results appeared, which are relevant to the analysis presented here.

(i) The WA85 Collaboration has measured at central rapidity the yield of Ω and $\overline{\Omega}$ in 200A GeV S-W collisions. From these results they now obtained the ratio $(\Omega+\overline{\Omega})/(\Xi+\overline{\Xi}) = 1.7 \pm 0.9$ (> 0.79 at the 95% confidence level) in a common $m_\perp$ range ($m_\perp > 2.3$ GeV/c^2) [44,45]. This rather large value is within the range of predictions made in Sec. III F 1 (see in particular Fig. 4).

(ii) The NA35 Collaboration [46] has given the ratio $\overline{\Lambda}/\bar{p} = 0.8 \pm 0.3$ for the system S-Au at 200 GeV/c (full phase space coverage). This allows to estimate [47] the ratio of the $1/m_\perp\, dN/dm_\perp$ distributions (see Fig. 3) at fixed $m_\perp$ in the rapidity interval $3 < y < 4$ for $\overline{\Lambda}$ and $\bar{p}$ to be greater than unity—we obtained such large result, $1 < \overline{\Lambda}/\bar{p} < 1.2$, see Fig. 4(c) (note the values of γ_s shown in Table I). A still greater ratio $\overline{\Lambda}/\bar{p} = 1.5 \pm 0.4$ (full phase space) was measured for the S-S collision system, consistent with the corresponding analysis [25].

These results confirm the internal consistency of our analysis and support the concept of relative chemical equilibrium in the baryon sector developed in this paper.

Our data analysis work presented here has since continued:

(1) The analysis [29] of 15 GeV A collisions at the BNL Alternating Gradient Synchrotron (AGS) was completed. In particular the entropy content of the thermal fireball was determined—it is consistent with both hadronic gas as well as quark-gluon plasma matter fireballs being formed at this energy [48].

(2) The values of T and λ_q which arise in the present work from the analysis of the data were derived within a simple dynamical model assuming that initially a QGP plasma fireball is formed [49].

(3) The analysis of S-S collisions [25] led to a more refined model [50] which allows for variations of the chemical potentials as functions of rapidity. A *rapidity independent* vanishing strange quark chemical potential $\mu_s = 0$ and a large strangeness saturation factor $\gamma_s = 0.75$–1 is confirmed despite a strong variation of the baryochemical potential: $\mu_B = 130$ MeV is found at central rapidity, rising to about 350 MeV in the fragmentation regions.

(4) In this improved S-S analysis [50] the normalization of the pion spectrum indicates a strong deficit (factor 2.5) of the hadronic gas model entropy, favoring the QGP picture, as was also noted in another analysis of the S-W/Pb data [51].

ACKNOWLEDGMENTS

J.R. thanks his colleagues in Paris for their warm and personal hospitality. The work of U.H. and J.S. was supported by DFG, BMFT, and GSI. The collaboration between U.H. and J.R. was supported by NATO Collaborative Research Grant No. 910991. J.R. acknowledges partial support by DOE Grant No. DE-FG02-92ER40733. The work of J.S. was supported by the Freistaat Bayern. Finally, U.H. would like to thank the Institute of Theoretical Physics at the University of Santa Barbara, where part of this work was done, for their nice hospitality, and the NSF for financial support of this stay under Grant No. PHY89-04035. Laboratoire de Physique Théorique et Hautes Energies is Unité associée au CNRS UA 280.

[1] J. Rafelski, Phys. Rep. **88**, 331 (1982).
[2] P. Koch and J. Rafelski, Nucl. Phys. **A444**, 678 (1985).
[3] P. Koch, B. Müller, and J. Rafelski, Phys. Rep. **142**, 167 (1986).
[4] See *Quark Matter '91*, Proceedings of the Ninth International Symposium on Ultrarelativistic Nucleus-Nucleus Collisions, Gatlinburg, Tennessee, edited by T. C. Awes *et al.* [Nucl. Phys. **A544** (1992)].
[5] S. Abatzis *et al.*, Phys. Lett. B **270**, 123 (1991); **259**, 508 (1991).
[6] WA85 Collaboration, D. Evans, in *Quark Matter '93*, Proceedings of the Tenth International Conference on Ultrarelativistic Nucleus-Nucleus Collisions, Borlänge, Sweden, edited by H. A. Gustafsson *et al.* [Nucl. Phys. **A566** (1994)]; and (private communication); WA85 Collaboration, S. Abatzis *et al.*, Phys. Lett. B **316**, 615 (1993).
[7] NA35 Collaboration, J. Bartke *et al.*, Z. Phys. C **48**, 191 (1990).
[8] NA36 Collaboration, E. Andersen *et al.*, Phys. Lett. B **294**, 127 (1992).
[9] J. Sollfrank, P. Koch, and U. Heinz, Phys. Lett. B **253**, 256 (1991); Z. Phys. C **52**, 593 (1991).
[10] S. Wenig, Ph.D. thesis Frankfurt/M, 1990 [GSI Report No. GSI-90-23, 1990 (unpublished)]; and NA35 Collaboration, J. Bächler *et al.*, Phys. Rev. Lett. **72**, 1419 (1994).
[11] K. S. Lee, U. Heinz, and E. Schnedermann, Z. Phys. C **48**, 525 (1990); E. Schnedermann and U. Heinz, Phys. Rev. Lett. **69**, 2908 (1992); Phys. Rev. C **47**, 1738 (1993); E. Schnedermann, J. Sollfrank, and U. Heinz, in *Particle Production in Highly Excited Matter*, edited by H. H. Gutbrod and J. Rafelski (Plenum, New York, 1993), p. 175; Phys. Rev. C **48**, 2462 (1993).
[12] N. K. Glendenning and J. Rafelski, Phys. Rev. C **31**, 823 (1985).
[13] U. Heinz, K. S. Lee, and M. Rhoades-Brown, Mod. Phys. Lett. A **2**, 153 (1987); K. S. Lee, M. Rhoades-Brown, and U. Heinz, Phys. Rev. C **37**, 1452 (1988).
[14] J. Rafelski, Phys. Lett. B **190**, 167 (1987).
[15] J. Rafelski and A. Schnabel, in *Intersections Between*

Particle and Nuclear Physics (Third International Conference), edited by G. M. Bunce, AIP Conf. Proc. No. 176 (AIP, New York, 1988), p. 1086 (see in particular Fig. 1).
[16] H.-C. Eggers and J. Rafelski, Int. J. Mod. Phys. A **6**, 1067 (1991) (see in particular Fig. 8).
[17] N. J. Davidson, H. G. Miller, R. M. Quick, and J. Cleymans, Phys. Lett. B **255**, 105 (1991).
[18] J. Cleymans, in *Quark Matter '90*, Proceedings of the International Symposium, Menton, France, edited by J. P. Blaicot *et al.* [Nucl. Phys. A **525**, 205c (1991)].
[19] J. Rafelski, Phys. Lett. B **262**, 333 (1991); in *Quark Matter '91* [4], p. 279c, and references therein.
[20] J. Letessier, A. Tounsi, and J. Rafelski, Phys. Lett. B **292**, 417 (1992); in *Proceedings of the XXVI International Conference on High Energy Physics*, Dallas, Texas, 1992, edited by J. R. Sanford, AIP Conf. Proc. No. 272 (AIP, New York, 1993), p. 983.
[21] J. Cleymans and H. Satz, Z. Phys. C **57**, 135 (1993).
[22] J. Letessier, A. Tounsi, U. Heinz, J. Sollfrank, and J. Rafelski, Phys. Rev. Lett. **70**, 3530 (1993).
[23] J. Cleymans, K. Redlich, H. Satz, and E. Suhonen, Z. Phys. C **58**, 347 (1993). (We received this reference after submittal of the original version of this manuscript.)
[24] CERN-EMU05 Collaboration, Y. Takahashi *et al.* (private communication); (unpublished).
[25] J. Sollfrank, M. Gaździcki, U. Heinz, and J. Rafelski, Z. Phys. C **61**, 659 (1994).
[26] J. Rafelski and B. Müller, Phys. Rev. Lett. **48**, 1066 (1982).
[27] B. Petersson, in *Quark Matter '90* [18], p. 237c.
[28] See various contributions in *Quark Matter '93* [6].
[29] J. Rafelski and M. Danos, Phys. Rev. C **50**, 1684 (1994).
[30] C. M. Ko, M. Asakawa, and P. Lévai, Phys. Rev. C **46**, 1072 (1992).
[31] H. Sorge, M. Berenguer, H. Stöcker, and W. Greiner, Phys. Lett. B **289**, 6 (1992).
[32] R. Hagedorn, I. Montvay, and J. Rafelski, in *Hadronic Matter at Extreme Density*, edited by N. Cabibbo and L. Sertorio (Plenum, New York, 1980), p. 49.
[33] M. Kataja, J. Letessier, P. V. Ruuskanen, and A. Tounsi, Z. Phys. C **55**, 153 (1992).
[34] Particle Data Group, K. Hikasa *et al.*, Phys. Rev. D **45**, S1 (1992).
[35] K. S. Lee and U. Heinz, Phys. Rev. D **47**, 2068 (1993).
[36] J. Rafelski, H. Rafelski, and M. Danos, Phys. Lett. B **294**, 131 (1992).
[37] C. Greiner, P. Koch, and H. Stöcker, Phys. Rev. Lett. **58**, 1825 (1987); C. Greiner, D. H. Rischke, H. Stöcker, and P. Koch, Phys. Rev. D **38**, 2797 (1988).
[38] L. Csernai, N. S. Amelin, E. F. Staubo, and D. Strottman, Bergen University Report No. 1991-14, Table 4; (private communication).
[39] AFS-ISR Collaboration, T. Åkesson *et al.*, Nucl. Phys. **B246**, 1 (1984).
[40] E. Quercigh *et al.*, WA94 proposal, Report No. CERN/SPSLC 91-5 P257, 1991 (unpublished).
[41] T. S. Biró and J. Zimányi, Nucl. Phys. **A395**, 525 (1983).
[42] J. Rafelski and M. Danos, Phys. Lett. B **192**, 432 (1987).
[43] For an overview see J. Zimányi *et al.*, in *Particle Production in Highly Excited Matter* [11], p. 243.
[44] WA85 Collaboration, S. Abatzis *et al.*, Phys. Lett. B **316**, 615 (1993); WA85 Collaboration, F. Antinori *et al.*, in *Proceedings of the NATO-ARW on Hot Hadronic Matter*, edited by J. Letessier *et al.* (Plenum, New York, 1995).
[45] WA85 Collaboration, F. Antinori *et al.*, in *Proceedings of the Workshop on Strangeness '95*, Tucson, Arizona, 1995, edited by J. Rafelski *et al.* (AIP, New York, in press); WA85 Collaboration, S. Abatzis *et al.*, Phys. Lett. B (to be published).
[46] NA35 Collaboration, Th. Alber *et al.*, Z. Phys. C **64**, 195 (1994); NA35 Collaboration, J. Günther *et al.*, in *Quark Matter '95*, edited by A. Poskanzer *et al.* [Nucl. Phys. A (to be published)].
[47] M. Gaździcki and NA35 Collaboration (private communication).
[48] J. Letessier, J. Rafelski, and A. Tounsi, Phys. Lett. B **328**, 499 (1994).
[49] J. Letessier, J. Rafelski, and A. Tounsi, Phys. Lett. B **333**, 484 (1994).
[50] C. Slotta, J. Sollfrank, and U. Heinz, in *Proceedings of the Workshop on Strangeness '95* [45].
[51] J. Letessier, J. Rafelski, and A. Tounsi, Phys. Lett. B **321**, 394 (1994).